Since January 2020 Elsevier has created a COVID-19 resource centre with free information in English and Mandarin on the novel coronavirus COVID-19. The COVID-19 resource centre is hosted on Elsevier Connect, the company's public news and information website.

Elsevier hereby grants permission to make all its COVID-19-related research that is available on the COVID-19 resource centre - including this research content - immediately available in PubMed Central and other publicly funded repositories, such as the WHO COVID database with rights for unrestricted research re-use and analyses in any form or by any means with acknowledgement of the original source. These permissions are granted for free by Elsevier for as long as the COVID-19 resource centre remains active.

Reliability Engineering and System Safety 236 (2023) 109305

Contents lists available at ScienceDirect

Reliability Engineering and System Safety

journal homepage: www.elsevier.com/locate/ress

Reliability analysis of body sensor networks with correlated isolation groups

Guilin Zhao [a], Liudong Xing [b,c,*]

[a] School of Computing & Artificial Intelligence, Southwest Jiaotong University, China
[b] Electrical & Computer Engineering Department, University of Massachusetts, Dartmouth, USA
[c] Department of Computer Science & Engineering, Graphic Era Deemed to be University, Dehradun, India

ARTICLE INFO

Keywords:
Body sensor network
Combinatorial method
Correlation
Random isolation time
Reliability analysis

ABSTRACT

Body sensor networks (BSNs) are playing a crucial role in tackling arising challenges during the COVID-19 pandemic. This work contributes by modeling and analyzing the BSN reliability considering the effects of correlated functional dependence (FDEP) and random isolation time behavior. Particularly, the FDEP exists in BSNs where a relay is utilized to assist the communication between some biosensors and the sink device. When the relay malfunctions, the dependent biosensors may communicate directly with the sink for a limited, uncertain time. These biosensors then become isolated from the rest of the BSN when their remaining power depletes to the level insufficient to support the direct communication. Moreover, multiple biosensors sharing the same relay and a biosensor communicating with the sink via several alternative relays create correlations among different FDEP groups. In addition, the competition in the time domain exists between the local failure of the relay and the propagated failures of dependent biosensors. Both the correlation and competition complicate the reliability modeling and analysis of BSNs. This work proposes a combinatorial and analytical methodology to address both effects in the BSN reliability analysis. The proposed method is demonstrated using a detailed case study and verified using a continuous-time Markov chain method.

1. Introduction

Body sensor networks (BSNs), which monitor the physiological and metabolic parameters of the human body, play an essential role in tackling arising challenges during the COVID-19 pandemic [1,2]. For example, by detecting the health-related information (e.g., temperature, oxygen saturation (SpO_2), respiratory rate, and lung sounds), BSNs can monitor the populations at risk (such as caregivers and people working at airports and restaurants) and determine the priority of infected people [3]. A lower priority is determined for people who are in the early stages of coronavirus infection and need to be quarantined, and a higher one is determined for people who are with mild symptoms but may suddenly worsen and need emergency care [3,4]. Due to the life-critical nature of the BSN applications, reliability modeling and analysis are necessary when designing and operating a BSN system [3,5].

A BSN system contains several wearable biosensors for sensing and transmitting signals and a sink device for processing data acquired. The relayed communication, where biosensors usually communicate with the sink device through a relay, is typically used for the BSN system to improve the reliability, energy efficiency, and long-term sustainability of information delivery [6–8]. The relationship between the relay and its dependent biosensors is an example of the functional dependence (FDPE) behavior, which can lead to the competition in the time domain between the local failure (denoted by LF) of the relay and the propagated failures (denoted by PF) of corresponding dependent biosensors [9,10]. This work assumes the propagated failure with global effect (PFGE), where a PF crashes the whole BSN system once occurring. Specifically, biosensors can be subject to PFs (which damage the biosensor itself and other BSN components, e.g., malicious cyber-attacks from intelligent eavesdropper [11]) and LFs (which damage the biosensor itself, e.g., malfunction due to aging [12]). The BSN system status is different according to the occurrence sequence of the relay's LF and the dependent biosensors' PFs. If the LF of the relay occurs first, the failure isolation effect dominates, preventing PFs originating from the dependent biosensors from damaging the rest of the BSN system and at the same time preventing the isolated biosensors from contributing to the function of the BSN system. On the other hand, if the PFs of dependent biosensors occur first, the failure propagation effect dominates, causing extensive damages to the BSN system. In summary, the

* Corresponding author.
E-mail address: lxing@umassd.edu (L. Xing).

https://doi.org/10.1016/j.ress.2023.109305
Received 23 September 2022; Received in revised form 30 March 2023; Accepted 10 April 2023
Available online 11 April 2023
0951-8320/© 2023 Elsevier Ltd. All rights reserved.

Acronyms

BDD	binary decision diagram
BSN	body sensor network
CTMC	continuous-time Markov chain
FDEP	functional dependence
FT	fault tree
LF	local failure
ITE	isolation time event
NDC	non-dependent component
PDF	probability density function
PF	propagated failure
PFGE	propagated failure with global effect
TE	trigger event
TTI	time-to-isolation

Notations

$A \rightarrow B$	event of the event A occurring before the event B
iLF	event of LF of component i
iI	event that component i is isolated from the system within the mission time
iPF	event of PFGE of component i
I_{NDC}	set of NDCs
SR	event that the system is reliable
t	mission time
$CR(t)$	conditional probability that the system is reliable given that at least one NDC has PFGE
$f_{iLF}(t)$	PDF of time-to-LF of component i
$f_{iPF}(t)$	PDF of time-to-PF of component i
$f_{iI}(t)$	PDF of time-to-isolation of the dependent component i given the failure of its relay
m	the number of triggers
$P_u(t)$	probability that at least one NDC has PFGE
$q_{iL}(t)$	conditional probability that component i has LF given that no PFGE occurs to component i
$q_{iLF}(t)$	LF occurrence probability of component i
$q_{iPF}(t)$	PFGE occurrence probability of component i
$R(t)$	system reliability
TE_j	occurrence of the trigger event j
D_j	set of affected dependent components under TE_j
n_j	the number of components in D_j
$SPF_{j,k}$	set of components with PFGEs in D_j under $TE_{j,k}$
$p_{j,k}$	the number of component in $SPF_{j,k}$
$SNPF_{j,k}$	set of components without PFGEs in D_j under $TE_{j,k}$
$q_{j,k}$	the number of components in $SNPF_{j,k}$

failure propagation effect and the failure isolation effect may take place in the actual BSN operation. The effect that dominates the status of the BSN system is dependent on the competitions between the relay's LF and the dependent biosensors' PFs in the time domain. In addition to BSNs [13], such competitions have been explored in the operation of other systems, such as the flight control system of the aircraft [14], the electricity system [15], and the hydroelectric generation plant [16].

The system reliability analysis has been investigated for different types of competitions. For example, competitions between the degradation and the catastrophic failures were modeled based on different statistical failure modes (e.g., *s*-independent [17,18] or *s*-dependent [19–21]). Competing processes were investigated in the context of accelerated life tests in [22,23], system maintenance policies in [24,25], and the system size optimization in [26,27]. Competitions between the uncovered and covered fault modes of system components were studied as the imperfect fault coverage behavior in some studies [28–30]. Distinguishable from those works, the competition addressed in this paper is between the failure propagation and isolation effects.

Addressing the competing failure propagation and isolation effects has recently received lots of attentions. Combinatorial reliability analysis methods were proposed for binary state systems [31–33], multi-state systems [34], phased mission systems [35–37], and cascading systems [38,39]. A generalized stochastic Petri net method was proposed for modeling the reliability of a system where the stochastic dependencies exist among the system components [14]. However, most of the existing models assumed instantaneous isolation when the failure isolation effect takes place. In practice, the isolation may take random time to happen. Specifically, in the BSN, when the LF of the relay occurs first, the dependent biosensor can increase its transmission power to enable the direct communication with the sink. Before the biosensor's remaining power depletes to the level insufficient to support the direct contact, the biosensor can communicate with the sink device directly (i.e., is not isolated). The time that it takes to isolate the dependent biosensor is random and uncertain, depending on the battery's remaining power and the distance between the dependent biosensor and the sink device. With the consideration of the random isolation time, the failure propagation effect dominates if any PF of the dependent biosensor takes place before the relay's failure, or it happens after the relay's failure but before the remaining battery power in the biosensor becomes insufficient to support the direct communication to the sink node.

In [40], the random isolation time was first studied for BSN systems with independent FDEP groups. However, the correlated FDEP groups exist in many real-world systems [41–43], where multiple biosensors may share the same relay or a biosensor can communicate with the sink device via several alternative relays (for fault-tolerant routing), incurring correlations among multiple FDEP groups and thus further complicating the BSN reliability modeling and analysis. This paper advances the state of the art by suggesting a combinatorial and analytical methodology for modeling and analyzing the reliability of BSNs subject to competing failure propagation and isolation effects from multiple correlated FDEP groups and random isolation time.

The remainder of the paper is organized as follows: Section 2 introduces the preliminary method for addressing the single FDEP group with the random isolation time. Section 3 proposes a combinatorial approach for evaluating the reliability of BSN systems subject to correlated FDEP groups and random isolation time. Section 4 presents a step-by-step illustration of the proposed method using an example BSN system. Section 5 presents numerical results and analysis. Verification of correctness of the proposed method using the Markov-based method is also performed. Finally, Section 6 concludes the work and outlines future research directions.

2. Preliminary method for modeling FDEP with random isolation time

To model the FDEP relationship between the relay (referred to as the trigger) and the dependent biosensor with the random isolation time

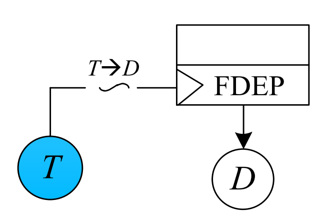

Fig. 1. Modeling FDEP with random isolation time.

behavior, an FDEP gate with a tilde symbol is defined as shown in Fig. 1, where T and D respectively model failure events of the trigger T and the dependent biosensor D, and $T \rightarrow D$ models that the biosensor D takes a random time to be isolated if the LF of the trigger T occurs.

As discussed in the Introduction, the competing behavior exists between the failure isolation and propagation effects. The failure isolation effect wins if T's LF happens before D's PFGE and the time needed for isolating D is less than the time difference between T's LF and D's PFGE. When the isolation effect wins, D is isolated and the BSN system may still be functional, depending on the components remaining in the system. The failure propagation effect wins if: i) D's PFGE happens before T's LF, or ii) D's PFGE happens after T's LF and the time needed for isolating D is greater than the time difference between them. When the failure propagation effect wins, D's PFGE crashes the entire system. Meanwhile, when T's LF occurs, it takes a random time for D to be isolated. Table 1 summarizes the occurrence of the isolation time behavior of D and the competing behavior based on the occurrence of T's LF (denoted by TLF) and D's PFGE (denoted by DPF). $\overline{TLF}$ and $\overline{DPF}$ are complementary events of TLF and DPF, respectively. Note that because we consider the isolation time behavior of the dependent biosensor D as the behavior that the dependent biosensor D takes a random time to be isolated given that TLF occurs and the competing behavior occurs when both TLF and DPF take place, in Table 1, neither the isolation time behavior nor the competing behavior happens under the combinations of $\overline{TLF} \cap \overline{DPF}$ and $\overline{TLF} \cap DPF$.

When the isolation time behavior of D happens, the system including the FDEP group may still function under three situations listed below.

- Situation (a): the system does not involve the competing behavior and the dependent component D is isolated after the mission time;
- Situation (b): the system does not involve the competing behavior and the dependent component D is isolated during the mission time; and
- Situation (c): the system involves the competing behavior and the dependent component D is isolated before DPF.

Fig. 2 illustrates the occurrence sequence of TLF, DPF, and DI under each situation, where DI denotes the event of D being isolated within the mission time given that TLF occurs (i.e., the failure isolation effect takes place).

The occurrence probability of each situation is calculated as follows. Under situations (a) and (b), no PFGE happens to D. Because the occurrence of the event DI depends only on the occurrence of the event TLF, the battery power remained in the dependent component D and the distance between D and the sink device, the relationship between the event DPF and the event DI is assumed to be independent. Note that while the failure propagation effect and the failure isolation effect are mutually exclusive, the relationship between the event DPF and the event TLF can be assumed to be independent since the two events occur to two different system components (i.e., the dependent component D experiencing the PFGE does not affect the trigger component T experiencing an LF and vice versa). Hence, the occurrence probability of situations (a) and (b), respectively denoted by $\Pr(TLF \cap \overline{DPF} \cap \overline{DI})$ and $\Pr(TLF \cap \overline{DPF} \cap DI)$, can be evaluated as (1) and (2), where $\Pr(\overline{DPF})$ is evaluated as $[1 - q_{DPF}(t)]$ with $q_{DPF}(t)$ denoting the PFGE occurrence probability of the dependent component D.

$$\Pr(TLF \cap \overline{DPF} \cap \overline{DI}) = \Pr(\overline{DPF}) \times \Pr(TLF \cap \overline{DI}) \tag{1}$$

$$\Pr(TLF \cap \overline{DPF} \cap DI) = \Pr(\overline{DPF}) \times \Pr(TLF \cap DI) \tag{2}$$

Suppose that TLF happens at τ_{TLF} and DI happens at τ_{DI}, $0 \le \tau_{TLF} \le t$ and $\tau_{TLF} \le \tau_{DI}$. The length of the time from the occurrence of TLF to the occurrence of DI, i.e., time-to-isolation (TTI), is denoted as τ_{TTI}, $\tau_{TTI} = \tau_{DI} - \tau_{TLF}$, and its interval is $[t - \tau_{TLF}, \infty]$ under situation (a) and is $[0, t - \tau_{TLF}]$ under situation (b). Based on the sequential event probability evaluation [16,44], $\Pr(TLF \cap \overline{DI})$ in (1) and $\Pr(TLF \cap DI)$ in (2) are obtained as (3), where $f_{TLF}(\tau_{TLF})$ is the probability density function (PDF) of time-to-LF of T at τ_{TLF}, and $f_{DI}(\tau_{TTI})$ is the PDF of TTI of D at τ_{DI} (i.e., the time when the event DI occurs) given that TLF occurs at τ_{TLF}.

$$\begin{aligned} \Pr(TLF \cap \overline{DI}) &= \int_0^t \int_{t-\tau_{TLF}}^{\infty} f_{TLF}(\tau_{TLF}) \times f_{DI}(\tau_{TTI}) d\tau_{TTI} d\tau_{TLF} \\ \Pr(TLF \cap DI) &= \int_0^t \int_0^{t-\tau_{TLF}} f_{TLF}(\tau_{TLF}) \times f_{DI}(\tau_{TTI}) d\tau_{TTI} d\tau_{TLF} \end{aligned} \tag{3}$$

Under situation (c), the competing failure behavior and the isolation time behavior occur. The FDEP model can be functional only if TLF occurs before DPF and the time needed for isolating D is less than the occurrence time between them (denotes by $\{(TLF \rightarrow DPF) \cap DI\}$). Suppose that TLF happens at τ_{TLF}, DPF happens at τ_{DPF}, and DI happens at τ_{DI}, $\tau_{TTI} = \tau_{DI} - \tau_{TLF}$, $0 \le \tau_{TLF} \le \tau_{DPF} \le t$ and $0 \le \tau_{TTI} \le \tau_{DPF} - \tau_{TLF}$. $\Pr(TLF \cap DPF \cap DI)$ is evaluated as (4), where $f_{TLF}(\tau_{TLF})$ is PDF of time-to-LF of T at τ_{TLF}, $f_{DPF}(\tau_{DPF})$ is the PDF of time-to-PFGE of D at τ_{DPF}, and $f_{DI}(\tau_{TTI})$ is the PDF of time-to-isolation of D at τ_{DI} given that TLF occurs at τ_{TLF}.

$$\begin{aligned} &\Pr(TLF \cap DPF \cap DI) = \Pr(\{(TLF \rightarrow DPF) \cap DI\}) \\ &\int_0^t \int_{\tau_{TLF}}^t \int_0^{\tau_{DPF}-\tau_{TLF}} f_{TLF}(\tau_{TLF}) \times f_{DPF}(\tau_{DPF}) \times f_{DI}(\tau_{TTI}) d\tau_{TTI} d\tau_{DPF} d\tau_{TLF} \end{aligned} \tag{4}$$

The model presented in this section aims to address the random isolation time behavior. Therefore, the FDEP group with a single trigger and a single dependent component is illustrated. This preliminary method is incorporated in the proposed methodology for addressing the FDEP model with multiple triggers and dependent components. Refer to Section 4 for specific illustrations.

3. Proposed combinatorial methodology

The combinatorial methodology proposed for the reliability analysis of BSNs with correlated FDEP groups and the random isolation time behavior contains five steps. Note that reliability is generally defined as "the probability that a product, system, process, or service will perform a required function under stated conditions for a stated period of time" [45]. In this work, the reliability of a BSN system is defined as the probability that the BSN system will perform its required monitoring function correctly using multiple biosensors and relays throughout an interval of time [0, t], where biosensors are used to measure physiological and/or motion information and relays are used to assist communications between biosensors and the sink device.

3.1. Step 1: separate PFGEs of non-dependent components

PFGEs originating from components whose functions are not dependent on any other system components' function cannot be isolated. Such components are referred to as non-dependent components (NDCs). Applying the total probability law, we can separate PFGEs of NDCs from the system reliability (denoted by $R(t)$) as (5), where SR represents that the system is reliable.

Table 1
The system behavior based on the occurrence of TLF and DPF.

Combinations	Behavior involved
$\overline{TLF} \cap \overline{DPF}$	Neither the isolation time behavior nor the competing behavior
$\overline{TLF} \cap DPF$	Neither the isolation time behavior nor the competing behavior
$TLF \cap \overline{DPF}$	The isolation time behavior only
$TLF \cap DPF$	Both the isolation time behavior and the competing behavior

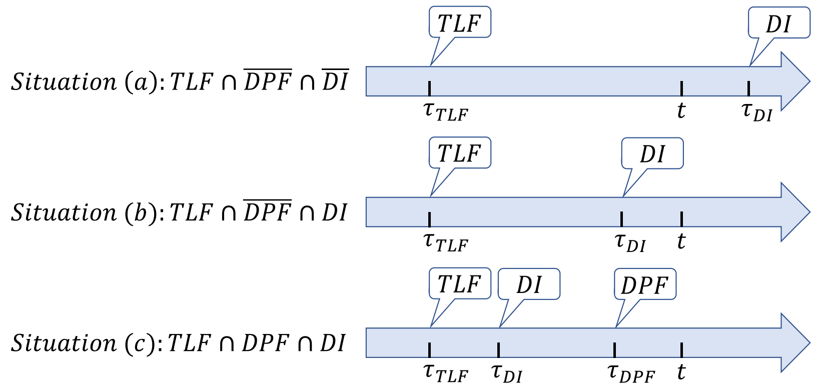

Fig. 2. Occurrence sequence of *TLF, DPF,* and *DI* under each situation.

$$R(t) = \Pr(SR|\textit{at least one NDC having PFGE}) \times \Pr(\textit{at least one NDC having PFGE}) + \Pr(SR|\textit{no NDCs having PFGEs}) \times \Pr(\textit{no NDCs having PFGEs}) \tag{5}$$

In (5), $\Pr(SR|\textit{at least one NDC having PFGE})$ is 0 since any PFGEs originating from NDCs can lead to the failure of the whole system. Denoting $\Pr(SR|\textit{no NDCs having PFGEs})$ by $CR(t)$ and $\Pr(\textit{no NDCs having PFGEs})$ by $P_u(t)$, (5) is simplified to (6).

$$R(t) = CR(t) \times P_u(t) \tag{6}$$

In (6), $P_u(t)$ is calculated by (7), where I_{NDC} denotes the set of NDCs subject to PFGEs and $q_{iPF}(t)$ denotes the PFGE occurrence probability of component i at time t and is evaluated based on the input time-to-PFGE parameters of component i.

$$P_u(t) = \prod_{\forall i \in I_{NDC}} [1 - q_{iPF}(t)] \tag{7}$$

The calculating procedure of $CR(t)$ is presented in steps 2 to 5 in Sections 3.2 – 3.5. Note that $CR(t)$ is a conditional probability. Therefore, the corresponding component i's failure probability used in calculating $CR(t)$, denoted by $q_{iL}(t)$, is a conditional failure probability given that component i does not experience PFGE. Considering the s-relationship between LF and PFGE of component i, $q_{iL}(t)$ is calculated by (8), where *iLF* and *iPF* are events of component i having an LF and a PFGE, respectively.

$$q_{iL}(t) = \Pr(iLF|\overline{iPF}) = \frac{\Pr(iLF \cap \overline{iPF})}{\Pr(\overline{iPF})} = \begin{cases} \dfrac{\Pr(iLF) \times \Pr(\overline{iPF})}{\Pr(\overline{iPF})} = q_{iLF}(t) \ \textit{independent LF and PFGE}, \\ \dfrac{\Pr(iLF)}{\Pr(\overline{iPF})} = \dfrac{q_{iLF}(t)}{1 - q_{iPF}(t)} \ \textit{mutually exclusive LF and PFGE}. \end{cases} \tag{8}$$

In (8), the independent relationship between LF and PFGE implies that the incidence of one event does not affect the occurrence probability of the other event, thus we have $\Pr(iLF \cap \overline{iPF}) = \Pr(iLF) \times \Pr(\overline{iPF})$. The mutually exclusive relationship represents that LF and PFGE are disjoint and cannot occur at the same time. Thus, we have $\Pr(iLF \cap \overline{iPF}) = \Pr(iLF)$ [46]. Note that each biosensor considered in this work is subject to LFs that may compromise its sensing function (referred to as sensing LF) or transmission function (referred to as transmission LF) [13]. If the PFGE of the same biosensor is caused by the jamming attacks that are based on the transmission function by transmitting illegal signals without compromising the sensing function of the biosensor, the relationship is independent between PFGE and sensing LF and is mutually exclusive between PFGE and transmitting LF.

3.2. Step 2: generate trigger event space

In the BSN system having m triggers, which are denoted as $T_1, \ldots, T_w, \ldots, T_m$, a trigger event space of 2^m disjoint sets can cover all possible combinations of the occurrence or non-concurrence of LFs of triggers. Denoting the occurrence and non-concurrence of LF of T_w by T_wLF and $\overline{T_wLF}$ respectively, one can enumerate each combination of trigger events (TEs) as shown in (9).

$$\begin{aligned} TE_1 &= \overline{T_1LF} \cap \overline{T_2LF} \cap \ldots \cap \overline{T_{m-1}LF} \cap \overline{T_mLF} \\ TE_2 &= T_1LF \cap \overline{T_2LF} \cap \ldots \cap \overline{T_{m-1}LF} \cap \overline{T_mLF} \\ &\vdots \\ TE_{2^m} &= T_1LF \cap T_2LF \cap \ldots \cap T_{m-1}LF \cap T_mLF \end{aligned} \tag{9}$$

Applying the total probability law, $CR(t)$ is calculated as

$$CR(t) = \sum_{j=1}^{2^m} \Pr(SR \cap TE_j). \tag{10}$$

To calculate $\Pr(SR \cap TE_j)$ in (10), two cases (Case 1 and Case 2) are considered based on the logic input of the FDEP gate.

Case 1. The inputs of all the FDEP gates are logic false ('0'), implying that either none of the triggers' LFs happen or the triggers' LFs happen but have no effect on the dependent components. Under Case 1, neither the competing failure behavior nor the isolation time behavior affects the BSN system. Applying the total probability law, $\Pr(SR \cap TE_j)$ under this case is calculated as (11), where $\Pr(TE_j)$ is determined by its definition in (9). $\Pr(SR|TE_j)$ is determined by the reduced fault tree (FT) model under TE_j, which is obtained by reducing the original system FT model through removing all the trigger failure events with the efficient binary decision diagram (BDD) based method [47]. $\Pr(SR \cap TE_j)$ under Case 1 is evaluated in this step.

$$\Pr(SR \cap TE_j) = \Pr(SR|TE_j) \times \Pr(TE_j) \tag{11}$$

Case 2. At least one of the inputs of the FDEP gates is logic true ('1'), i.e., the LF of the trigger happens and affects the related dependent components. Under this case, the competing failure behavior and/or the isolation time behavior occur(s) to the BSN system. Applying the divide-and-conquer principle, we divide $\Pr(SR \cap TE_j)$ under Case 2 by addressing these two behaviors in Step 3.

3.3. Step 3: analyze competing failure behavior and isolation time behavior under Case 2

Under TE_j, suppose that the set of affected dependent components is D_j and the number of them is n_j, i.e., $D_j = \{D_{j1}, \ldots D_{jx}, \ldots D_{jn_j}\}$. Based on the occurrence or non-concurrence of D_{jx}'s PFGE (respectively denoted by $D_{jx}PF$ and $\overline{D_{jx}PF}$), a dependent component event space is generated. Each combination (denoted by $TE_{j,k}, k = 1, 2, \cdots, 2^{n_j}$) is enumerated as shown in (12).

$$
\begin{aligned}
TE_{j,1} &= \overline{D_{j1}PF} \cap \overline{D_{j2}PF} \cap \ldots \cap \overline{D_{j(n_j-1)}PF} \cap \overline{D_{jn_j}PF} \\
TE_{j,2} &= D_{j1}PF \cap \overline{D_{j2}PF} \cap \ldots \cap \overline{D_{j(n_j-1)}PF} \cap \overline{D_{jn_j}PF} \\
&\vdots \\
TE_{j,2^{n_j}} &= D_{j1}PF \cap D_{j2}PF \cap \ldots \cap D_{j(n_j-1)}PF \cap D_{jn_j}PF
\end{aligned} \tag{12}
$$

Applying the total probability law, $\Pr(SR \cap TE_j)$ under Case 2 can be calculated by

$$
\Pr(SR \cap TE_j) = \sum_{k=1}^{2^{n_j}} \Pr(SR \cap TE_{j,k}). \tag{13}
$$

Consider $TE_{j,k}$. Denote the number of affected dependent components (i.e., components in D_j) that have PFGEs as $p_{j,k}$ and they constitute the set $SPF_{j,k}$, and denote the number of components in D_j that have no PFGEs as $q_{j,k}$ and they constitute the set $SNPF_{j,k}$. Based on the definition of $TE_{j,k}$ in (12), $p_{j,k}$, $q_{j,k}$, $SPF_{j,k}$, and $SNPF_{j,k}$ are summarized in Table 2.

According to the values of $p_{j,k}$ and $q_{j,k}$, Case 2 can be further divided into three scenarios: (a) $p_{j,1} = 0,\ q_{j,1} = n_j$ (i.e., $TE_{j,1}$); (b) $p_{j,k} = n_j, q_{j,k} = 0$ (i.e., $TE_{j,2^{n_j}}$); and (c) $p_{j,k} \neq 0, q_{j,k} \neq 0$ (i.e., $TE_{j,k}, k = 2, \cdots, 2^{n_j} - 1$).

The isolation time behavior is involved when calculating $\Pr(SR \cap TE_{j,k})$. Specifically, it is incorporated with the competing failure behavior for components in $SPF_{j,k}$ and is considered without the competing failure behavior for components in $SNPF_{j,k}$. The analysis procedures for $TE_{j,1}$, $TE_{j,2^{n_j}}$, and $TE_{j,k}, k = 2, \cdots, 2^{n_j} - 1$ are performed as follows.

$TE_{j,1}$: $p_{j,1} = 0$, $q_{j,1} = n_j$, $SPF_{j,1} = \varnothing$, and $SNPF_{j,1} = \{D_{j,1,x} | D_{j1}, D_{j2}, \cdots, D_{jn_j}, x = 1, 2, \cdots, n_j\}$. Since $SPF_{j,1}$ is empty, the competing failure behavior does not exist. The isolation time behavior is addressed for $D_{j,1,x}$ in $SNPF_{j,1}$. According to the isolation status of $D_{j,1,x}$, an isolation time event (ITE) space is generated. It contains 2^{n_j} mutually exclusive ITEs as shown in (14), where $D_{j,1,x}I$ and $\overline{D_{j,1,x}I}$ represents $D_{j,1,x}$'s isolation and $D_{j,1,x}$'s non-isolation, respectively. Applying the total probability law, $\Pr(SR \cap TE_{j,1})$ in (13) can be calculated by (15).

$$
\begin{aligned}
ITE_{j,1,1} &= \overline{D_{j,1,1}I} \cap \overline{D_{j,1,2}I} \cap \ldots \cap \overline{D_{j,1,(n_j-1)}I} \cap \overline{D_{j,1,n_j}I} \\
ITE_{j,1,2} &= D_{j,1,1}I \cap \overline{D_{j,1,2}I} \cap \ldots \cap \overline{D_{j,1,(n_j-1)}I} \cap \overline{D_{j,1,n_j}I} \\
&\vdots \\
ITE_{j,1,2^{n_j}} &= D_{j,1,1}I \cap D_{j,1,2}I \cap \ldots \cap D_{j,1,(n_j-1)}I \cap D_{j,1,n_j}I
\end{aligned} \tag{14}
$$

Table 2
$p_{j,k}, q_{j,k}$, $SPF_{j,k}$, and $SNPF_{j,k}$ for $TE_{j,k}$, $k = 1, 2, \cdots, 2^{n_j}$.

	$p_{j,k}$	$q_{j,k}$	$SPF_{j,k}$	$SNPF_{j,k}$
$k = 1$	0	n_j	$\varnothing$	$\{D_{j1}, D_{j2}, \cdots, D_{jn_j}\}$
$k = 2$	1	$n_j - 1$	$\{D_{j1}\}$	$\{D_{j2}, \cdots, D_{jn_j}\}$
…	…	…	…	…
$k = 2^{n_j}$	n_j	0	$\{D_{j1}, D_{j2}, \cdots, D_{jn_j}\}$	$\varnothing$

$$
\begin{aligned}
\Pr(SR \cap TE_{j,1}) &= \sum_{l=1}^{2^{n_j}} \Pr(SR \cap TE_{j,1} \cap ITE_{j,1,l}) \\
&= \sum_{l=1}^{2^{n_j}} \Pr(SR | TE_{j,1} \cap ITE_{j,1,l}) \times \Pr(TE_{j,1} \cap ITE_{j,1,l})
\end{aligned} \tag{15}
$$

$TE_{j,2^{n_j}}$: According to Table 2, $p_{j,2^{n_j}} = n_j$, $q_{j,2^{n_j}} = 0$, $SPF_{j,2^{n_j}} = \{D_{j,2^{n_j},y} | D_{j1}, D_{j2}, \cdots, D_{jn_j}, y = 1, 2, \cdots, n_j\}$, and $SNPF_{j,2^{n_j}} = \varnothing$. Since $SPF_{j,2^{n_j}}$ is not empty, the competing failure behavior occurs, which is caused by the different occurrence sequences of TE_j (defined in (9)) and the PFGE of $D_{j,2^{n_j},y}$ in the time domain. The competing results and related requirements are introduced in Section 2. Note that under $TE_{j,2^{n_j}}$, D and T in Section 2 are revised to $D_{j,2^{n_j},y}$ and TE_j, respectively. Denote the event of the failure propagation dominating the BSN system as $TE_{j,2^{n_j},p}$ with subscript p being the propagation effect and the event of the failure isolation dominating as $TE_{j,2^{n_j},i}$ with subscript i being the isolation effect. $\Pr(SR \cap TE_{j,2^{n_j}})$ in (13) is calculated and simplified as

$$
\begin{aligned}
&\Pr(SR \cap TE_{j,2^{n_j}}) = \Pr(SR \cap TE_{j,2^{n_j},p}) + \Pr(SR \cap TE_{j,2^{n_j},i}) \\
&= \Pr(SR | TE_{j,2^{n_j},p}) \times \Pr(TE_{j,2^{n_j},p}) + \Pr(SR | TE_{j,2^{n_j},i}) \times \Pr(TE_{j,2^{n_j},i}) \\
&= \Pr(SR | TE_{j,2^{n_j},i}) \times \Pr(TE_{j,2^{n_j},i}).
\end{aligned} \tag{16}
$$

$TE_{j,k}$, $k = 2, 3, \cdots, 2^{n_j} - 1$: According to Table 2, $p_{j,k} \neq 0$, $q_{j,k} \neq 0$, $SPF_{j,k} \neq \varnothing$, and $SNPF_{j,k} \neq \varnothing$. Consider $SPF_{j,k} = \{D_{j,k,y} | D_{j1}, \ldots, D_{jy}, y = 1, \cdots, p_{j,k}\}$ and $SNPF_{j,k} = \{D_{j,k,x} | D_{j1}, \ldots, D_{jx}, x = 1, \cdots, q_{j,k}\}$. The competing failure behavior and the isolation time behavior affect $D_{j,k,y}$ and the isolation time behavior affects $D_{j,k,x}$. The competing result is either the failure propagation (denoted by $TE_{j,k,p}$) or the failure isolation (denoted by $TE_{j,k,i}$). An ITE space is generated to cover $2^{q_{j,k}}$ mutually exclusive combinations. Combining the analyzing procedure of $TE_{j,1}$ and $TE_{j,2^{n_j}}$, $\Pr(SR \cap TE_{j,k})$ in (13) is obtained by (17).

$$
\begin{aligned}
&\Pr(SR \cap TE_{j,k}) = \Pr(SR \cap TE_{j,k,p}) + \Pr(SR \cap TE_{j,k,i}) \\
&= \sum_{m=1}^{2^{q_{j,k}}} \Pr(SR \cap TE_{j,k,p} \cap ITE_{j,k,m}) + \sum_{m=1}^{2^{q_{j,k}}} \Pr(SR \cap TE_{j,k,i} \cap ITE_{j,k,m}) \\
&= \sum_{m=1}^{2^{q_{j,k}}} \left[\Pr(SR | TE_{j,k,p} \cap ITE_{j,k,m}) \times \Pr(TE_{j,k,p} \cap ITE_{j,k,m})\right] \\
&+ \sum_{m=1}^{2^{q_{j,k}}} \left[\Pr(SR | TE_{j,k,i} \cap ITE_{j,k,m}) \times \Pr(TE_{j,k,i} \cap ITE_{j,k,m})\right] \\
&= \sum_{m=1}^{2^{q_{j,k}}} \left[\Pr(SR | TE_{j,k,i} \cap ITE_{j,k,m}) \times \Pr(TE_{j,k,i} \cap ITE_{j,k,m})\right]
\end{aligned} \tag{17}
$$

$\Pr(TE_{j,1} \cap ITE_{j,1,l}), l = 1, 2, \cdots, 2^{n_j}$ in (15), $\Pr(TE_{j,2^{n_j},i})$ in (16), and $\Pr(TE_{j,k,i} \cap ITE_{j,k,m})$, $m = 1, 2, \cdots, 2^{q_{j,k}}$ in (17) can be evaluated by applying the preliminary method in Section 2 with components' input time-to-LF/PFGE parameters and components' input isolation time parameters. Refer to Section 4.2.3 for illustrations. $\Pr(SR | TE_{j,1} \cap ITE_{j,1,l}), l = 1, 2, \cdots, 2^{n_j}$ in (15), $\Pr(SR | TE_{j,2^{n_j},i})$ in (16), and $\Pr(SR | TE_{j,k,i} \cap ITE_{j,k,m})$, $m = 1, 2, \cdots, 2^{q_{j,k}}$ in (17) are evaluated in the next step.

3.4. Step 4: evaluate conditional system reliability

$\Pr(SR | TE_{j,1} \cap ITE_{j,1,l})$ denotes the conditional system reliability given that the dependent components indicated by $ITE_{j,1,l}$ are isolated by the occurrence of $TE_{j,1}$. For example, when $l = 2$, according to (14), $D_{j,1,1}$ is isolated. Similarly, $\Pr(SR | TE_{j,2^{n_j},i})$ in (16) and $\Pr(SF | TE_{j,k,i} \cap ITE_{j,k,m})$ in (17) denote the conditional system reliability given the isolation of the dependent components under $TE_{j,2^{n_j},i}$ and $TE_{j,k,i} \cap ITE_{j,k,m}$, respectively. These conditional system reliabilities can be evaluated by applying the efficient BDD-based method on the reduced FT model [47], which is obtained by removing the trigger failure events and replacing all isolated dependent components with constant '1' (True). Refer to Section 4.2.4 for illustrations.

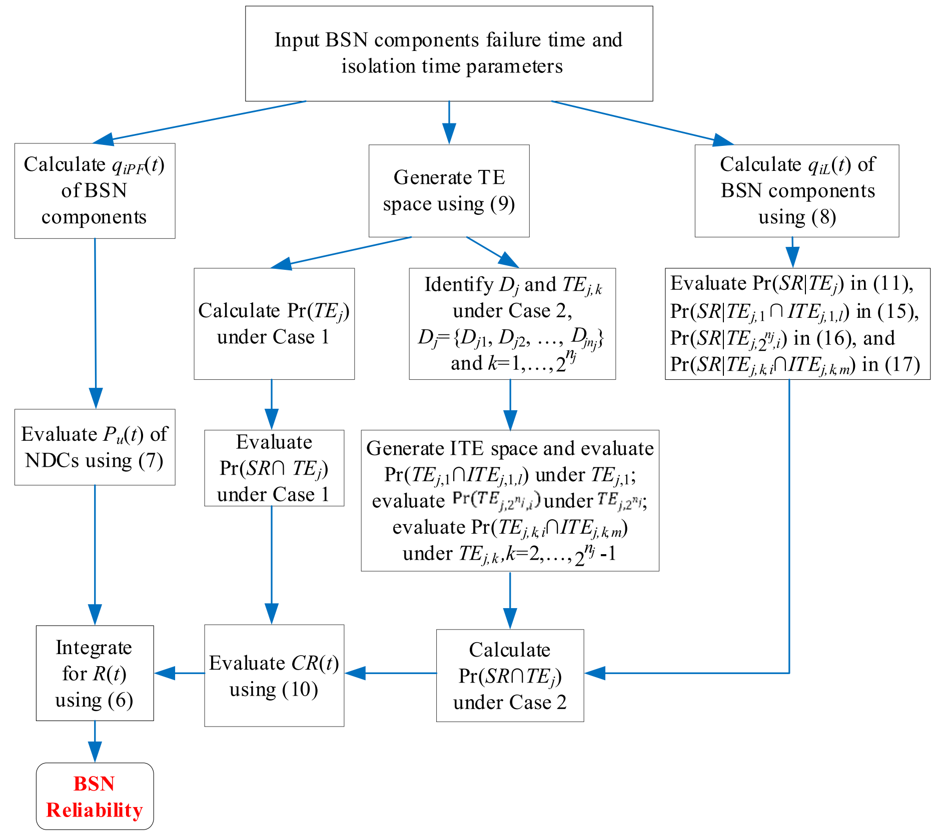

Fig. 3. Flowchart for the proposed BSN reliability evaluation method.

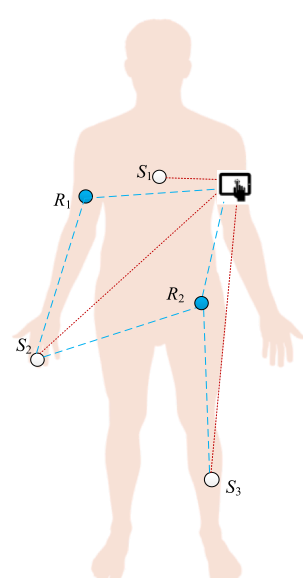

Fig. 4. Example patient monitoring BSN system.

3.5. Step 5: integrate for the entire system reliability

$\Pr(SR \cap TE_j)$ under Case 1 is obtained by (11) in Step 2. According to (14), $\Pr(SR \cap TE_j)$ under Case 2 is obtained in Step 3 by (13) via integrating $\Pr(SR \cap TE_{j,1})$ evaluated by (15), $\Pr(SR \cap TE_{j,2^{n_j}})$ evaluated by (16), and $\Pr(SR \cap TE_{j,k}), k = 2, \cdots, 2^{n_j} - 1$ evaluated by (17). Having $\Pr(SR \cap TE_j)$ under both Cases 1 and 2, $CR(t)$ is consecutively obtained by (10). Finally, with $P_u(t)$ obtained by (7), the entire BSN system reliability is integrated using (6).

Based on discussions in Sections 3.1–3.5, Fig. 3 shows the flowchart of the proposed BSN reliability evaluation algorithm.

4. Illustrative example

Fig. 4 shows an example patient monitoring BSN system, which consists of three biosensors (S_1, S_2, and S_3) and two relays (R_1 and R_2). Specifically, sensors S_1 and S_2 are used to measure patient's physiological information like heart rates and oxygen saturation (SpO_2); sensor S_3 is the motion sensor and is used to track patient's body positions. Sensor S_1 can communicate with the sink device directly. Sensor S_2 can deliver sensed data to the sink device via R_1 or R_2. Sensor S_3 can deliver sensed data to the sink device via R_2. The sink device gathers and processes the data acquired by all the sensors, facilitating caregivers' involvement in

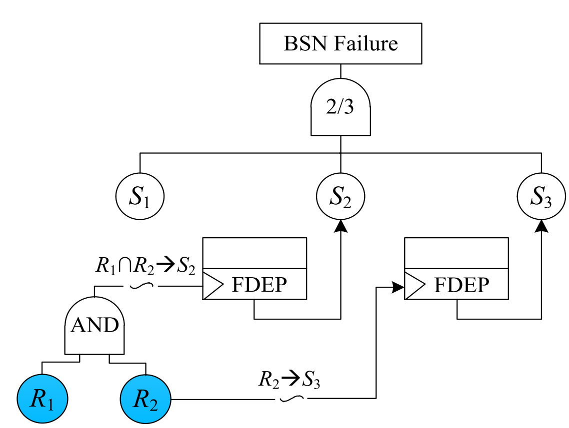

Fig. 5. Dynamic FT model of the example BSN system.

action taking. The sink device is assumed to be perfect during the considered mission time.

4.1. FT modeling

Fig. 5 illustrates the dynamic FT model of the example BSN system. To obtain a good diagnostic certainty, the caregiver requires at least two types of information; in other words, the example BSN system fails when any two out of three biosensors malfunction, which is modeled using the top 2-out-of-3 gate in the system dynamic FT.

The FDEP behavior with random isolation time exists among relays (R_1 and R_2) and biosensors (S_2 and S_3) in the illustrative example. In the case where R_1 and R_2 undergo LFs, S_2 and S_3 can communicate with the sink directly within a certain period (modeled by random isolation time); as time goes on, remaining power in respective biosensor depletes to the level insufficient to support the direct link, resulting in biosensor (s) becoming inaccessible/isolated from the system. To model the FDEP behavior, two FDEP gates are used for the two correlated FDEP groups. The left FDEP group involves R_1, R_2, S_2, and a top AND gate connecting R_1 and R_2, which models S_2 depending on either R_1 or R_2. The right FDEP group involves R_2 and S_3. To model the random isolation time behavior, $R_1 \cap R_2 \rightarrow S_2$ denotes that S_2 takes a random time to be isolated when R_1 and R_2 fail, and $R_2 \rightarrow S_3$ denotes that S_3 takes a random time to be isolated when R_2 fails.

Note that various approaches (e.g., Markov models [48], Monte Carlo simulations [49], stochastic approaches [50], and fuzzy approaches [51]) may be applied to analyze dynamic FT models (without considering the competing failure isolation and propagation effects). In this work, we perform the dynamic FT analysis using the proposed combinatorial methodology to evaluate the reliability of BSN systems subject to the competing behavior.

4.2. Step by step analysis

To evaluate the example BSN reliability, i.e., $R(t)$ in (6), the procedure proposed in Section 3 is applied. The detailed analysis is performed step by step in Sections 4.2.1 – 4.2.5.

4.2.1. Step 1: separate PFGEs of non-dependent biosensors

Applying (6), the PFGE effect of NDCs is separated. For the illustrated BSN system, $I_{NDC} = \{R_1, R_2, S_1\}$. Based on (7), $P_u(t)$ is evaluated as (18). The evaluating procedure of $CR(t)$ in (6) is elaborated in the following subsections (Sections 4.2.2 – 4.2.5).

$$P_u(t) = \left(1 - q_{R_1PF}(t)\right) \times \left(1 - q_{R_2PF}(t)\right) \times \left(1 - q_{S_1PF}(t)\right) \tag{18}$$

4.2.2. Step 2: generate trigger event space

In the example BSN system, there are two triggers. Therefore, $T_1 = R_1$, $T_2 = R_2$, and $m = 2$. The example system contains $2^2 = 4$ TEs. Applying (9), each TE is defined as shown Table 3. Applying (10), $CR(t)$ is obtained as (19).

$$CR(t) = \sum_{j=1}^{4} \Pr\left(SR \cap TE_j\right) \tag{19}$$

Table 3
Definition and classification of TE_j, $j = 1,2,3,4$.

	Definition	Inputs of FDEP groups	Classification
$j = 1$	$\overline{R_1LF} \cap \overline{R_2LF}$	'0' for both FDEP groups	Case 1
$j = 2$	$R_1LF \cap \overline{R_2LF}$	'0' for both FDEP groups	Case 1
$j = 3$	$\overline{R_1LF} \cap R_2LF$	'0' for the left FDEP group and '1' for the right FDEP group	Case 2
$j = 4$	$R_1LF \cap R_2LF$	'1' for both FDEP groups	Case 2

According to logic inputs of each FDEP group, TE_1 and TE_2 are classified into Case 1, and TE_3 and TE_4 are classified into Case 2. $\Pr(SR \cap TE_1)$ and $\Pr(SR \cap TE_2)$ are evaluated in this step; $\Pr(SR \cap TE_3)$ and $\Pr(SR \cap TE_4)$ are evaluated in Step 3.

TE_1: Applying (11), $\Pr(SR \cap TE_1)$ is evaluated as (20), where $\Pr(TE_1)$ is determined by its definition in Table 3 as (21).

$$\Pr(SR \cap TE_1) = \Pr(SR|TE_1) \times \Pr(TE_1) \tag{20}$$

$$\begin{aligned} \Pr(TE_1) &= \Pr(\overline{R_1LF} \cap \overline{R_2LF}) = \Pr(\overline{R_1LF}) \times \Pr(\overline{R_2LF}) \\ &= \left[1 - q_{R_1L}(t)\right] \times \left[1 - q_{R_2L}(t)\right] \end{aligned} \tag{21}$$

Under TE_1, both R_1 and R_2 function correctly, and neither the competing failure behavior nor the isolation time behavior occurs to S_2 and S_3. The reduced system FT model for evaluating $\Pr(SR|TE_1)$ is given in Fig. 6(a), which is generated by removing R_1, R_2, and all the FDEP gates from the FT model in Fig. 5. The reduced FT model under TE_1 contains the biosensors undergoing PFGEs, therefore, the separable method formulated in (6) is applied to calculate $\Pr(SR|TE_1)$ as (22), where $P_{u-TE_1}(t)$ denotes the occurrence probability of no PFGEs originating from biosensors under TE_1 and is evaluated as (23). Note that S_1's PFGE effect is excluded when calculating $P_{u-TE_1}(t)$ since it has been considered in (18).

$CR_{TE_1}(t)$ in (22) denotes the conditional system reliability given that no PFGEs originate from biosensors in the reduced FT model. To convert the FT model to the BDD model, the 2-out-of-3 gate is expanded to a set of AND and OR gates as shown in Fig. 6(b). Using the operations rules in [47], the corresponding BDD model is gendered as shown in Fig. 6(c), where the 0-edge of each non-sink node is marked with the solid green line, representing that the corresponding component is reliable; the 1-edge is marked with the dashed red line, representing that the corresponding component is failed. Therefore, $CR_{TE_1}(t)$ is evaluated as (24) by adding all paths' probabilities from the root node S_1 to the sink node '0' in the BDD model.

$$\Pr(SR|TE_1) = R_{TE_1}(t) = CR_{TE_1}(t) \times P_{u-TE_1}(t) \tag{22}$$

$$P_{u-TE_1}(t) = \left[1 - q_{S_2PF}(t)\right] \times \left[1 - q_{S_3PF}(t)\right] \tag{23}$$

$$\begin{aligned} CR_{TE_1}(t) = &\left[1-q_{S_1L}(t)\right] \times \left[1-q_{S_2L}(t)\right] + \left[1-q_{S_1L}(t)\right] \times q_{S_2L}(t) \times \left[1-q_{S_3L}(t)\right] \\ &+ q_{S_1L}(t) \times \left[1-q_{S_2L}(t)\right] \times \left[1-q_{S_3L}(t)\right] \end{aligned} \tag{24}$$

TE_2: Applying (11), $\Pr(SR \cap TE_2)$ is evaluated as (25), where $\Pr(TE_2)$ is determined by its definition in Table 3 as $q_{R_1L}(t) \times [1 - q_{R_2L}(t)]$.

$$\Pr(SR \cap TE_2) = \Pr(SR|TE_2) \times \Pr(TE_2) \tag{25}$$

Under TE_2, R_1 fails locally and R_2 functions correctly. Since R_1's LF has no effect on S_2 and S_3, neither the competing failure behavior nor the isolation time behavior occurs to the BSN system. The reduced system FT model for evaluating $\Pr(SR|TE_2)$ is obtained by removing R_1, R_2, and all the FDEP gates, which is the same as that in Fig. 6(a). Therefore, $\Pr(SR|TE_2)$ is the same as $\Pr(SR|TE_1)$, i.e., $\Pr(SR|TE_2) = \Pr(SR|TE_1)$.

4.2.3. Step 3: analyze competing failure behavior and isolation time behavior under Case 2

According to Table 3, TE_3 and TE_4 are under Case 2. The competing failure behavior and the isolation time behavior under TE_3 and TE_4 are analyzed in Sections 4.2.3.1 and 4.2.3.2 as follows.

4.2.3.1. TE3.

R_1 functions correctly and R_2 fails locally, resulting in S_3 being affected. Therefore, the set of the affected dependent biosensor under TE_3 is $D_3 = \{S_3\}$ and the number of the affected dependent biosensor is $n_3 = 1$. Based on (12), the dependent biosensor event space has $2^1 = 2$ combinations, which are $TE_{3,1} = \overline{S_3PF}$ and $TE_{3,2} = S_3PF$. Applying (13), $\Pr(SR \cap TE_3)$ in (19) is obtained by

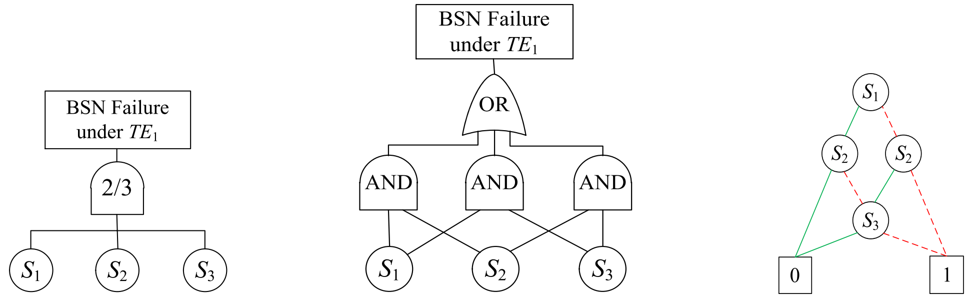

(a) reduced FT model (b) expended FT model (c) BDD model

Fig. 6. Reduced system models under TE_1.

Table 4
Definition, $p_{3,k}, q_{3,k}$, $SPF_{3,k}$, and $SNPF_{3,k}$ under $TE_{3,k}$, $k = 1, 2$.

	Definition	$p_{3,k}$	$q_{3,k}$	$SPF_{3,k}$	$SNPF_{3,k}$
$k = 1$	$\overline{S_3PF}$	0	1	$\varnothing$	$\{S_3\}$
$k = 2$	S_3PF	1	0	$\{S_3\}$	$\varnothing$

Table 5
Definition of $ITE_{3,1,l}$, $l = 1, 2$.

	Definition
$l = 1$	$\overline{S_3I}$
$l = 2$	S_3I

$$\Pr(SR \cap TE_3) = \sum_{k=1}^{2} \Pr(SR \cap TE_{3,k}). \tag{26}$$

The isolation time behavior of S_3 under $TE_{3,1}$ and $TE_{3,2}$ is addressed. Specifically, under $TE_{3,1}$, no PFGE originates from S_3; therefore, the number of affected dependent biosensors with PFGEs is 0, and the number of affected dependent biosensor without PFGEs is 1 and it forms the set $SNPF_{3,1}$, i.e., $p_{3,1} = 0$, $q_{3,1} = 1$, $SPF_{3,1} = \varnothing$, and $SNPF_{3,1} = \{S_3\}$. Under $TE_{3,2}$, PFGE originates from S_3, therefore, $p_{3,2} = 1$, $q_{3,2} = 0$, $SPF_{3,2} = \{S_3\}$, and $SNPF_{3,2} = \varnothing$. Table 4 summarizes the definition, $p_{3,k}$, $q_{3,k}$, $SPF_{3,k}$, and $SNPF_{3,k}$ under $TE_{3,k}$. The competing failure behavior and the isolation time behavior under each $TE_{3,k}$ are analyzed as follows.

$TE_{3,1}$: No PFGE originates from S_3 and R_2 fails locally; therefore, the competing failure behavior does not exist and the isolation time behavior of S_3 is addressed. Applying (14), the ITE space under $TE_{3,1}$ is generated and shown in Table 5. Applying (15), $\Pr(SR \cap TE_{3,1})$ in (26) is evaluated as (27), where $\Pr(TE_{3,1} \cap ITE_{3,1,l})$ is evaluated in this step and $\Pr(SR|TE_{3,1} \cap ITE_{3,1,l})$ is evaluated in Step 4 (refer to Section 4.2.4.1).

$$\Pr(SR \cap TE_{3,1}) = \sum_{l=1}^{2} \Pr(SR|TE_{3,1} \cap ITE_{3,1,l}) \times \Pr(TE_{3,1} \cap ITE_{3,1,l}) \tag{27}$$

$TE_{3,1} \cap ITE_{3,1,1}$: S_3 is not isolated from the system. According to defined TE_3 (Table 3), $TE_{3,1}$ (Table 4), and $ITE_{3,1,1}$ (Table 5), $\Pr(TE_{3,1} \cap ITE_{3,1,1})$ denotes the occurrence probability of the event $\{\overline{R_1LF} \cap R_2LF \cap \overline{S_3PF} \cap \overline{S_3I}\}$. Since events $\overline{R_1LF}$, $\overline{S_3PF}$, and $(R_2LF \cap \overline{S_3I})$ are assumed to be independent, $\Pr\{\overline{R_1LF} \cap R_2LF \cap \overline{S_3PF} \cap \overline{S_3I}\}$ can be calculated as $[\Pr(\overline{R_1LF}) \times \Pr(\overline{S_3PF}) \times \Pr(R_2LF \cap \overline{S_3I}\}]$. Applying the first equation of (3) in Section 2 with the time-to-LF parameters of R_2 and the isolation time parameters of S_3, $\Pr(TE_{3,1} \cap ITE_{3,1,1})$ is obtained as

$$\Pr(TE_{3,1} \cap ITE_{3,1,1}) = [1 - q_{R_1L}(t)] \times [1 - q_{S_3PF}(t)] \times \int_0^t \int_{\tau_{R_2L}}^{\infty} f_{R_2L}(\tau_{R_2L}) f_{S_3I}(\tau_{TTI}) d\tau_{TTI} d\tau_{R_2L} \tag{28}$$

$TE_{3,1} \cap ITE_{3,1,2}$: S_3 is isolated from the system. $\Pr(TE_{3,1} \cap ITE_{3,1,2})$ denotes the occurrence probability of the event $\{\overline{R_1LF} \cap R_2LF \cap \overline{S_3PF} \cap S_3I\}$. Applying the second equation of (3), it is obtained as

$$\Pr(TE_{3,1} \cap ITE_{3,1,2}) = [1 - q_{R_1L}(t)] \times [1 - q_{S_3PF}(t)] \times \int_0^t \int_0^{t-\tau_{R_2L}} f_{R_2L}(\tau_{R_2L}) f_{S_3I}(\tau_{TTI}) d\tau_{TTI} d\tau_{R_2L} \tag{29}$$

$TE_{3,2}$: Since PFGE originates from S_3, the competing failure behavior and the isolation time behavior take effect on S_3. Based on Table 4, $p_{3,2} = 1$, $q_{3,2} = 0$, $SPF_{3,2} = \{S_3\}$, and $SNPF_{3,2} = \varnothing$. According to the competing result, two disjoint events are distinguished:

- $TE_{3,2,i}$: R_2LF happens before S_3PF, and the time for isolating S_3 is less than the difference between them. The example BSN system may still be alive depending on S_2 and S_3.
- $TE_{3,2,p}$: S_3PF happens before R_2LF, or S_3PF happens after R_2LF and the time needed for isolating S_3 is greater than the time difference between the occurrence time of R_2LF and S_3PF. The entire BSN system fails.

Applying (16), we have (30), where $\Pr(TE_{3,2,i})$ is evaluated in this step and $\Pr(SR|TE_{3,2,i})$ is evaluated in Step 4 (refer to Section 4.2.4.1.).

$$\Pr(SR \cap TE_{3,2}) = \Pr(SR|TE_{3,2,i}) \times \Pr(TE_{3,2,i}) \tag{30}$$

According to the definition of TE_3 (Table 3) and $TE_{3,2,i}$, $\Pr(TE_{3,2,i})$ denotes the occurrence probability of the event $\{\overline{R_1LF} \cap [(R_2LF \rightarrow S_3PF) \cap S_3I]\}$. Since the events $\overline{R_1LF}$ and $[(R_2LF \rightarrow S_3PF) \cap S_3I]$ are assumed to be independent, $\Pr\{\overline{R_1LF} \cap [(R_2LF \rightarrow S_3PF) \cap S_3I]\}$ is evaluated as $\Pr\{\overline{R_1LF}\} \times \Pr\{(R_2LF \rightarrow S_3PF) \cap S_3I\}$. Applying (4) with the input time-to-LF parameters of R_2, the input time-to-PFGE and isolation time parameters of S_3, $\Pr(TE_{3,2,i})$ is evaluated as

$$\Pr(TE_{3,2,i}) = [1 - q_{R_1L}(t)] \times \left[\int_0^t \int_{\tau_{R_2L}}^t \int_0^{\tau_{S_3PF} - \tau_{R_2L}} f_{R_2L}(\tau_{R_2L}) f_{S_3PF}(\tau_{S_3PF}) f_{S_3I}(\tau_{TTI}) d\tau_{TTI} d\tau_{S_3PF} d\tau_{R_2L} \right]. \tag{31}$$

4.2.3.2. TE$_4$. Both R_1 and R_2 fail locally, resulting in S_2 and S_3 being affected. Therefore, $D_4 = \{S_2, S_3\}$ and $n_4 = 2$. Based on (12), the dependent biosensor event space has four combinations. The definition,

Table 6
Definition, $p_{4,k}$, $q_{4,k}$, $SPF_{4,k}$, and $SNPF_{4,k}$ under $TE_{4,k}$, $k = 1, 2, 3, 4$.

	Definition	$p_{4,k}$	$q_{4,k}$	$SPF_{4,k}$	$SNPF_{4,k}$
$k = 1$	$\overline{S_2PF} \cap \overline{S_3PF}$	0	2	$\varnothing$	$\{S_2, S_3\}$
$k = 2$	$S_2PF \cap \overline{S_3PF}$	1	1	$\{S_2\}$	$\{S_3\}$
$k = 3$	$\overline{S_2PF} \cap S_3PF$	1	1	$\{S_3\}$	$\{S_2\}$
$k = 4$	$S_2PF \cap S_3PF$	2	0	$\{S_2, S_3\}$	$\varnothing$

Table 7
Definition of $ITE_{4,1,l}$, $l = 1, 2, 3, 4$.

	Definition
$l = 1$	$\overline{S_2I} \cap \overline{S_3I}$
$l = 2$	$S_2I \cap \overline{S_3I}$
$l = 3$	$\overline{S_2I} \cap S_3I$
$l = 4$	$S_2I \cap S_3I$

$p_{4,k}$, $q_{4,k}$, $SPF_{4,k}$, and $SNPF_{4,k}$ of each combination are given in Table 6. Applying (13), $\Pr(SR \cap TE_4)$ in (19) is calculated as (32). The competing failure behavior and the isolation time behavior under each $TE_{4,k}$ are analyzed as follows.

$$\Pr(SR \cap TE_4) = \sum_{k=1}^{4} \Pr(SR \cap TE_{4,k}) \tag{32}$$

$TE_{4,1}$: R_1 and R_2 fail locally and no PFGE originates from S_2 or S_3; therefore, the isolation time behavior of S_2 and S_3 is addressed but the competing failure behavior does not exist. Applying (14) with $p_{4,1}$, $q_{4,1}$, $SPF_{4,1}$, and $SNPF_{4,1}$ given in Table 6, the ITE space under $TE_{4,1}$ is generated and shown in Table 7. Applying (15), $\Pr(SR \cap TE_{4,1})$ is obtained as (33), where $\Pr(TE_{4,1} \cap ITE_{4,1,l})$ is evaluated as follows and $\Pr(SR|TE_{4,1} \cap ITE_{4,1,l})$ is evaluated in Step 4 (refer to Section 4.2.4.2.).

$$\Pr(SR \cap TE_{4,1}) = \sum_{l=1}^{4} \Pr(SR|TE_{4,1} \cap ITE_{4,1,l}) \times \Pr(TE_{4,1} \cap ITE_{4,1,l}) \tag{33}$$

$TE_{4,1} \cap ITE_{4,1,l}$: The definition and the formula for evaluating $\Pr(TE_{4,1} \cap ITE_{4,1,l})$ are summarized in Table 8. Take $\Pr(TE_{4,1} \cap ITE_{4,1,1})$ (i.e., $\Pr\{R_1LF \cap R_2LF \cap \overline{S_2PF} \cap \overline{S_3PF} \cap \overline{S_2I} \cap \overline{S_3I}\}$) as an example. Since no PFGEs originate from S_2 and S_3 under $TE_{4,1}$, it is evaluated as $\Pr\{\overline{S_2PF}\} \times \Pr\{\overline{S_3PF}\} \times \Pr\{R_1LF \cap R_2LF \cap \overline{S_2I} \cap \overline{S_3I}\}$ with $\Pr\{\overline{S_2PF}\} = [1 - q_{S_2PF}(t)]$ and $\Pr\{\overline{S_3PF}\} = [1 - q_{S_3PF}(t)]$. $\Pr\{R_1LF \cap R_2LF \cap \overline{S_2I} \cap \overline{S_3I}\}$ is evaluated by the preliminary method. Specifically, there are two possible occurrence sequences between R_1LF and R_2LF, which are either R_1LF before R_2LF (denoted by $R_1LF \rightarrow R_2LF$) or R_2LF before R_1LF (denoted by $R_2LF \rightarrow R_1LF$). Therefore, $\Pr\{R_1LF \cap R_2LF \cap \overline{S_2I} \cap \overline{S_3I}\}$ equals to the summation of $[\Pr\{(R_1LF \rightarrow R_2LF) \cap \overline{S_2I} \cap \overline{S_3I}\}$ and $\Pr\{(R_2LF \rightarrow R_1LF) \cap \overline{S_2I} \cap \overline{S_3I}\}]$. Suppose that R_1LF happens at τ_{R_1L}, R_2LF happens at τ_{R_2L}, S_2I happens at τ_{S_2I}, and S_3I happens at τ_{S_3I}. In terms of the event $(R_1LF \rightarrow R_2LF) \cap \overline{S_2I} \cap \overline{S_3I}$, we have $0 \le \tau_{R_1L} \le \tau_{R_2L} \le t$, $\tau_{R_2L} \le \tau_{S_2I}$, and $\tau_{R_2L} \le \tau_{S_3I}$. According to the BSN system configuration, the event S_2I happens when $R_1LF \cap R_2LF$ occurs and the event S_3I happens when R_2LF occurs. Based on (3), the interval is $[t - \tau_{R_2L}, \infty]$ of τ_{TTI-S_2} (which is the difference of τ_{S_2I} and τ_{R_2L}) and is $[t - \tau_{R_2L}, \infty]$ of τ_{TTI-S_3} (which is the difference of τ_{S_3I} and τ_{R_2L}). In terms of the event $(R_2LF \rightarrow R_1LF) \cap \overline{S_2I} \cap \overline{S_3I}$, $0 \le \tau_{R_2L} \le \tau_{R_1L} \le t$, $\tau_{R_1L} \le \tau_{S_2I}$, and $\tau_{R_2L} \le \tau_{S_3I}$, the interval is $[t - \tau_{R_1LF}, \infty]$ of τ_{TTI-S_2} (which is the difference of τ_{S_2I} and τ_{R_1L}) and is $[t - \tau_{R_2LF}, \infty]$ of τ_{TTI-S_3} (which is the difference of τ_{S_3I} and τ_{R_2L}). In summary, $\Pr(TE_{4,1} \cap ITE_{4,1,1})$ is evaluated as (34). $\Pr(TE_{4,1} \cap ITE_{4,1,l}), l = 2, 3, 4$ can be obtained via the same analysis procedure.

$$\begin{aligned}&\Pr(TE_{4,1} \cap ITE_{4,1,1}) = [1 - q_{S_2PF}(t)] \times [1 - q_{S_3PF}(t)] \times \\ &\Big[\int_0^t \int_{\tau_{R_1L}}^t \int_{t-\tau_{R_2L}}^{\infty} \int_{t-\tau_{R_2L}}^{\infty} f_{R_1L}(\tau_{R_1L}) f_{R_2L}(\tau_{R_2L}) f_{S_2I}(\tau_{TTI-S_2}) \times \\ &f_{S_3I}(\tau_{TTI-S_3}) d\tau_{TTI-S_3} d\tau_{TTI-S_2} d\tau_{R_2L} d\tau_{R_1L} \\ &\int_0^t \int_{\tau_{R_2L}}^t \int_{t-\tau_{R_1L}}^{\infty} \int_{t-\tau_{R_2L}}^{\infty} f_{R_2L}(\tau_{R_2L}) f_{R_1L}(\tau_{R_1L}) f_{S_2I}(\tau_{TTI-S_2}) \times \\ &f_{S_3I}(\tau_{TTI-S_3}) d\tau_{TTI-S_3} d\tau_{TTI-S_2} d\tau_{R_1L} d\tau_{R_2L}\Big]\end{aligned} \tag{34}$$

Table 9
Definition of $ITE_{4,2,m}$, $m = 1, 2$.

	Definition
$m = 1$	$\overline{S_3I}$
$m = 2$	S_3I

$TE_{4,2}$: R_1 and R_2 fail locally, PFGE originates from S_2, and no PFGE originates from S_3; therefore, the competing failure behavior and the isolation time behavior affect S_2 and the isolation time behavior of S_3 is addressed. Based on the competing result, two disjoint events ($TE_{4,2,p}$ and $TE_{4,2,i}$) are distinguished. According to the isolation status of S_3, two ITEs are generated and shown in Table 9. Applying (17), $\Pr(SR \cap TE_{4,2})$ is obtained as (35), where $\Pr(TE_{4,2,i} \cap ITE_{4,2,m}), m = 1, 2$ is evaluated in this step and $\Pr(SR|TE_{4,2,i} \cap ITE_{4,2,m})$ is evaluated in Step 4.

$$\Pr(SR \cap TE_{4,2}) = \sum_{m=1}^{2} \left[\Pr(SR|TE_{4,2,i} \cap ITE_{4,2,m}) \times \Pr(TE_{4,2,i} \cap ITE_{4,2,m})\right] \tag{35}$$

$TE_{4,2,i} \cap ITE_{4,2,m}$: When $m = 1$, $\Pr(TE_{4,2,i} \cap ITE_{4,2,1})$ denotes the occurrence probability of the event $\{R_1LF \cap R_2LF \cap S_2PF \cap \overline{S_3PF} \cap S_2I \cap \overline{S_3I}\}$, and it is calculated as $\Pr\{\overline{S_3PF}\} \times \Pr\{R_1LF \cap R_2LF \cap S_2PF \cap S_2I \cap \overline{S_3I}\}$ with $\Pr\{\overline{S_3PF}\} = [1 - q_{S_3PF}(t)]$ and $\Pr\{R_1LF \cap R_2LF \cap S_2PF \cap S_2I \cap \overline{S_3I}\} = [\Pr\{(R_1LF \rightarrow R_2LF \rightarrow S_2PF) \cap S_2I \cap \overline{S_3I}\} + \Pr\{(R_2LF \rightarrow R_1LF \rightarrow S_2PF) \cap S_2I \cap \overline{S_3I}\}]$. Applying the preliminary method, $\Pr(TE_{4,2,i} \cap ITE_{4,2,1})$ is evaluated as (36). Similarly, $\Pr(TE_{4,2,i} \cap ITE_{4,2,2})$ is evaluated as (37).

$$\begin{aligned}&\Pr(TE_{4,2,i} \cap ITE_{4,2,1}) = [1 - q_{S_3PF}(t)] \\ &\times \Big[\int_0^t \int_{\tau_{R_1L}}^t \int_{\tau_{R_2L}}^t \int_0^{\tau_{S_2PF}-\tau_{R_2L}} \int_{t-\tau_{R_2L}}^{\infty} f_{R_1L}(\tau_{R_1L}) f_{R_2L}(\tau_{R_2L}) f_{S_2PF}(\tau_{S_2PF}) \\ &\times f_{S_2I}(\tau_{TTI-S_2}) f_{S_3I}(\tau_{TTI-S_3}) d\tau_{TTI-S_3} \cdots d\tau_{R_1L} \\ &+ \int_0^t \int_{\tau_{R_2L}}^t \int_{\tau_{R_1L}}^t \int_0^{\tau_{S_2PF}-\tau_{R_1L}} \int_{t-\tau_{R_2L}}^{\infty} f_{R_2L}(\tau_{R_2L}) f_{R_1L}(\tau_{R_1L}) f_{S_2PF}(\tau_{S_2PF}) \\ &\times f_{S_2I}(\tau_{TTI-S_2}) f_{S_3I}(\tau_{TTI-S_3}) d\tau_{TTI-S_3} \cdots d\tau_{R_2L}\Big]\end{aligned} \tag{36}$$

Table 8
Definition and formula for evaluating $\Pr(TE_{4,1} \cap ITE_{4,1,l})$, $l = 1, 2, 3, 4$.

Event	Definition	$\Pr(TE_{4,1} \cap ITE_{4,1,l})$
$TE_{4,1} \cap ITE_{4,1,1}$	$\{R_1LF \cap R_2LF \cap \overline{S_2PF} \cap \overline{S_3PF} \cap \overline{S_2I} \cap \overline{S_3I}\}$	$\Pr(\overline{S_2PF}) \times \Pr(\overline{S_3PF}) \times \begin{bmatrix}\Pr\{(R_1LF \rightarrow R_2LF) \cap \overline{S_2I} \cap \overline{S_3I}\} + \\ \Pr\{(R_2LF \rightarrow R_1LF) \cap \overline{S_2I} \cap \overline{S_3I}\}\end{bmatrix}$
$TE_{4,1} \cap ITE_{4,1,2}$	$\{R_1LF \cap R_2LF \cap \overline{S_2PF} \cap \overline{S_3PF} \cap S_2I \cap \overline{S_3I}\}$	$\Pr(\overline{S_2PF}) \times \Pr(\overline{S_3PF}) \times \begin{bmatrix}\Pr\{(R_1LF \rightarrow R_2LF) \cap S_2I \cap \overline{S_3I}\} + \\ \Pr\{(R_2LF \rightarrow R_1LF) \cap S_2I \cap \overline{S_3I}\}\end{bmatrix}$
$TE_{4,1} \cap ITE_{4,1,3}$	$\{R_1LF \cap R_2LF \cap \overline{S_2PF} \cap \overline{S_3PF} \cap \overline{S_2I} \cap S_3I\}$	$\Pr(\overline{S_2PF}) \times \Pr(\overline{S_3PF}) \times \begin{bmatrix}\Pr\{(R_1LF \rightarrow R_2LF) \cap \overline{S_2I} \cap S_3I\} + \\ \Pr\{(R_2LF \rightarrow R_1LF) \cap \overline{S_2I} \cap S_3I\}]\end{bmatrix}$
$TE_{4,1} \cap ITE_{4,1,4}$	$\{R_1LF \cap R_2LF \cap \overline{S_2PF} \cap \overline{S_3PF} \cap S_2I \cap S_3I\}$	$\Pr(\overline{S_2PF}) \times \Pr(\overline{S_3PF}) \times \begin{bmatrix}\Pr\{(R_1LF \rightarrow R_2LF) \cap S_2I \cap S_3I\} + \\ \Pr\{(R_2LF \rightarrow R_1LF) \cap S_2I \cap S_3I\}\end{bmatrix}$

Table 10
Formula for evaluating $\Pr(TE_{4,3,i} \cap ITE_{4,3,m}),\ m = 1, 2$.

Event	Definition	$\Pr(TE_{4,3,i} \cap ITE_{4,3,m})$
$TE_{4,3,i} \cap ITE_{4,3,1}$	$R_1LF \cap R_2LF \cap \overline{S_2PF} \cap S_3PF \cap \overline{S_2I} \cap S_3I\}$	$\Pr(\overline{S_2PF}) \times \begin{bmatrix} \Pr(R_1LF \to R_2LF \to S_3PF) \cap S_3I \cap \overline{S_2I})+ \\ \Pr(R_2LF \to R_1LF \to S_3PF) \cap S_3I \cap \overline{S_2I})+ \\ \Pr(R_2LF \to S_3PF \to R_1LF) \cap S_3I \cap \overline{S_2I}) \end{bmatrix}$
$TE_{4,3,i} \cap ITE_{4,3,2}$	$R_1LF \cap R_2LF \cap \overline{S_2PF} \cap S_3PF \cap S_2I \cap S_3I\}$	$\Pr(\overline{S_2PF}) \times \begin{bmatrix} \Pr(R_1LF \to R_2LF \to S_3PF) \cap S_3I \cap S_2I)+ \\ \Pr(R_2LF \to R_1LF \to S_3PF) \cap S_3I \cap S_2I)+ \\ \Pr(R_2LF \to S_3PF \to R_1LF) \cap S_3I \cap S_2I) \end{bmatrix}$

$$\begin{aligned} &\Pr\left(TE_{4,2,i} \cap ITE_{4,2,2}\right) = \left[1 - q_{S_3PF}(\mathrm{t})\right] \\ &\times \left[\int_0^t \int_{\tau_{R_1L}}^t \int_{\tau_{R_2L}}^t \int_0^{\tau_{S_2PF}-\tau_{R_2L}} \int_0^{t-\tau_{R_2L}} f_{R_1L}(\tau_{R_1L}) f_{R_2L}(\tau_{R_2L}) f_{S_2PF}(\tau_{S_2PF}) \right. \\ &\times f_{S_2I}(\tau_{TTI-S_2}) f_{S_3I}\left(\tau_{TTI-S_3}\right) d\tau_{TTI-S_3} \cdots d\tau_{R_1L} \\ &+ \int_0^t \int_{\tau_{R_2L}}^t \int_{\tau_{R_1L}}^t \int_0^{\tau_{S_2PF}-\tau_{R_1L}} \int_0^{t-\tau_{R_2L}} f_{R_2L}(\tau_{R_2L}) f_{R_1L}(\tau_{R_1L}) f_{S_2PF}(\tau_{S_2PF}) \\ &\times f_{S_2I}(\tau_{TTI-S_2}) f_{S_3I}\left(\tau_{TTI-S_3}\right) d\tau_{TTI-S_3} \cdots d\tau_{R_2L} \end{aligned} \tag{37}$$

$TE_{4,3}$: R_1 and R_2 fail locally, no PFGE originates from S_2, and PFGE originates from S_3; therefore, the isolation time behavior of S_2 is addressed and the competing failure behavior and the isolation time behavior affect S_3. Two disjoint events ($TE_{4,3,i}$ and $TE_{4,3,p}$) are distinguished and two ITEs are generated ($ITE_{4,3,1} = \overline{S_2I}$, and $ITE_{4,3,2} = S_2I$). Applying (17), $\Pr(SR \cap TE_{4,3})$ is obtained as (38). The analysis procedure of $\Pr(TE_{4,3,i} \cap ITE_{4,3,m})$ is similar to that of $\Pr(TE_{4,2,i} \cap ITE_{4,2,m})$. Table 10 summarizes the formula for calculating $\Pr(TE_{4,3,i} \cap ITE_{4,3,m})$. $\Pr(SR|TE_{4,3,i} \cap ITE_{4,3,m})$ is evaluated in Step 4.

$$\Pr\left(SR \cap TE_{4,3}\right) = \sum_{m=1}^{2} \left[\Pr\left(SR|TE_{4,3,i} \cap ITE_{4,3,m}\right) \times \Pr\left(TE_{4,3,i} \cap ITE_{4,3,m}\right)\right] \tag{38}$$

$TE_{4,4}$: R_1 and R_2 fail locally and PFGEs originate from S_2 and S_3; therefore, the competing failure behavior and the isolation time behavior are addressed for S_2 and S_3. According to the competing result, two disjoint events ($TE_{4,4,i}$, and $TE_{4,4,p}$) are distinguished. Applying (16), we have (39), where $\Pr(SR|TE_{4,4,i})$ equals to 0 for the illustrative BSN system since both S_2 and S_3 are isolated under $TE_{4,4}$.

$$\Pr\left(SR \cap TE_{4,4}\right) = \Pr\left(SR\middle|TE_{4,4,i}\right) \times \Pr\left(TE_{4,4,i}\right) = 0 \tag{39}$$

4.2.4. Step 4: evaluate the conditional system reliability

This step illustrates the procedure for analyzing the conditional system reliabilities under TE_3 and TE_4, which are $\Pr(SR|TE_{3,1} \cap ITE_{3,1,l}), l = 1, 2$ in (27), $\Pr(SR|TE_{3,2,i})$ in (30), $\Pr(SR|TE_{4,1} \cap ITE_{4,1,l}), l = 1, 2, 3, 4$ in (33), $\Pr(SR|TE_{4,2,i} \cap ITE_{4,2,m}), m = 1, 2$ in (35), $\Pr(SR|TE_{4,3,i} \cap ITE_{4,3,m})$ $, m = 1, 2$ in (38), and $\Pr(SR|TE_{4,4,i})$ in (39).

4.2.4.1. TE_3. $TE_{3,1} \cap ITE_{3,1,l}, l = 1, 2$: The reduced FT and BDD models for evaluating $\Pr(SR|TE_{3,1} \cap ITE_{3,1,l})$ are obtained as follows. Under $TE_{3,1} \cap ITE_{3,1,1}$, the isolation time behavior of S_3 is addressed. But because the power in S_3 is sufficient to support the direct link between the sink and S_3 within the mission time, S_3 is not isolated (refer to the Situation (a) in Section 2), the failure of R_2 cannot cause the isolation of S_3 and S_3 remains in the BSN system. The reduced FT and BDD models under $TE_{3,1} \cap ITE_{3,1,1}$ are the same as those in Fig. 6. Under $TE_{3,1} \cap ITE_{3,1,2}$ (refer to Situation (b) in Section 2), the failure of R_2 causes the isolation of S_3. Therefore, the reduced FT model is obtained by replacing S_3 with '1', which is shown as Fig. 7(a). The corresponding BDD model is given in Fig. 7(b).

Table 11
$P_{u-TE_{3,1} \cap ITE_{3,1,l}}(t)$ and $CR_{TE_{3,1} \cap ITE_{3,1,l}}(t),\ l = 1, 2$.

l	$P_{u-TE_{3,1} \cap ITE_{3,1,l}}(t)$	$CR_{TE_{3,1} \cap ITE_{3,1,l}}(t)$
1	$[1 - q_{S_2PF}(t)]$	$CR_{TE_1}(t)$
2	$[1 - q_{S_2PF}(t)]$	$[1 - q_{S_1L}(t)] \times [1 - q_{S_2L}(t)]$

Using the similar separable method formulated in (6), $\Pr(SR|TE_{3,1} \cap ITE_{3,1,l})$ is evaluated as (40), where $P_{u-TE_{3,1} \cap ITE_{3,1,l}}(t)$ denotes the occurrence probability of no PFGEs originating from biosensors appearing in the reduced FT model (excluding S_1 considered in (18) and S_3 considered in (28) or (29)). $CR_{TE_{3,1} \cap ITE_{3,1,l}}(t)$ denotes the conditional system reliability given that no PFGEs originate from biosensors in the reduced FT model under $TE_{3,1} \cap ITE_{3,1,l}$ and can be obtained by the BDD-based method. The evaluation expressions of $CR_{TE_{3,1} \cap ITE_{3,1,l}}(t)$ and $P_{u-TE_{3,1} \cap ITE_{3,1,l}}(t)$ are summarized in Table 11. Note that $CR_{TE_{3,1} \cap ITE_{3,1,1}}(t)$ equals to $CR_{TE_1}(t)$ as they have the identical reduced FT and BDD models.

$$\Pr\left(SR|TE_{3,1} \cap ITE_{3,1,l}\right) = CR_{TE_{3,1} \cap ITE_{3,1,l}}(t) \times P_{u-TE_{3,1} \cap ITE_{3,1,l}}(t) \tag{40}$$

$TE_{3,2,i}$: The competing failure behavior occurs between R_2LF and S_3PF, and the competing result is S_3 being isolated from the BSN system. Therefore, the reduced FT model is generated by removing all the relays and the FDEP gates from the dynamic FT model and replacing S_3 with '1'. The reduced FT and BDD models under $TE_{3,2,i}$ are the same as those in Fig. 7. Using the similar separable method formulated in (6), $\Pr(SR|TE_{3,2,i})$ is evaluated as

$$\begin{aligned} &\Pr\left(SR|TE_{3,2,i}\right) = CR_{TE_{3,2,i}}(t) \times P_{u-TE_{3,2,i}}(t) \\ &= \left[1 - q_{S_1L}(t)\right] \times \left[1 - q_{S_2L}(t)\right] \times \left[1 - q_{S_2PF}(t)\right]. \end{aligned} \tag{41}$$

(a) reduced FT model

(b) BDD model

Fig. 7. Reduced system models under $TE_{3,1} \cap ITE_{3,1,2}$.

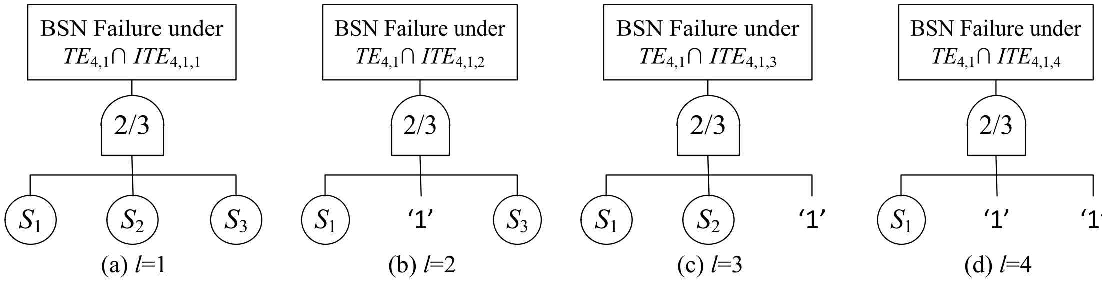

Fig. 8. Reduced system FT models under $TE_{4,1} \cap ITE_{4,1,l},\ l = 1,2,3,4$.

Table 12
$P_{u-TE_{4,1}\cap ITE_{4,1,l}}(t)$ and $CR_{TE_{4,1}\cap ITE_{4,1,l}}(t),\ l = 1,2,3,4$.

l	$P_{u-TE_{4,1}\cap ITE_{4,1,l}}(t)$	$CR_{TE_{4,1}\cap ITE_{4,1,l}}(t)$
1	1	$CR_{TE_1}(t)$
2	1	$[1 - q_{S_1L}(t)] \times [1 - q_{S_3L}(t)]$
3	1	$[1 - q_{S_1L}(t)] \times [1 - q_{S_2L}(t)]$
4	–	0

Table 13
$P_{u-TE_{4,2,i}\cap ITE_{4,2,m}}(t)$ and $CR_{TE_{4,2,i}\cap ITE_{4,2,m}}(t),\ m = 1,2$.

m	$P_{u-TE_{4,2,i}\cap ITE_{4,2,m}}(t)$	$CR_{TE_{4,2,i}\cap ITE_{4,2,m}}(t)$
1	1	$[1 - q_{S_1L}(t)] \times [1 - q_{S_3L}(t)]$
2	–	0

Table 14
$P_{u-TE_{4,3,i}\cap ITE_{4,3,m}}(t)$ and $CR_{TE_{4,3,i}\cap ITE_{4,3,m}}(t),\ m = 1,2$.

m	$P_{u-TE_{4,3,i}\cap ITE_{4,3,m}}(t)$	$CR_{TE_{4,3,i}\cap ITE_{4,3,m}}$
1	1	$[1 - q_{S_1L}(t)] \times [1 - q_{S_2L}(t)]$
2	–	0

4.2.4.2. TE_4. $TE_{4,1} \cap ITE_{4,1,l}, l = 1,2,3,4$: The reduced FT models for evaluating $\Pr(SR|TE_{4,1} \cap ITE_{4,1,l})$ are shown in Fig. 8. Using the same analysis procedure, the expressions for evaluating $CR_{TE_{4,1}\cap ITE_{4,1,l}}(t)$ and $P_{u-TE_{4,1}\cap ITE_{4,1,l}}(t)$ are summarized in Table 12. Correspondingly, we have $\Pr(SR|TE_{4,1} \cap ITE_{4,1,l}) = CR_{TE_{4,1}\cap ITE_{4,1,l}}(t) \times P_{u-TE_{4,1}\cap ITE_{4,1,l}}(t)$.

$TE_{4,2,i} \cap ITE_{4,2,m}$, $m = 1, 2$: The reduced system FT models under events $TE_{4,2,i} \cap ITE_{4,2,1}$ and $TE_{4,2,i} \cap ITE_{4,2,2}$ are identical to the models in Fig. 8(b) and (d), respectively. Based on the reduced FT models, $CR_{TE_{4,2,i}\cap ITE_{4,2,m}}(t)$ and $P_{u-TE_{4,2,i}\cap ITE_{4,2,m}}(t)$ are summarized in Table 13. We have $\Pr(SR|TE_{4,2,i} \cap ITE_{4,2,m}) = CR_{TE_{4,2,i}\cap ITE_{4,2,m}}(t) \times P_{u-TE_{4,2,i}\cap ITE_{4,2,m}}(t)$.

$TE_{4,3,i} \cap ITE_{4,3,m}$, $m = 1, 2$: The reduced FT models under events $TE_{4,3,i} \cap ITE_{4,3,1}$ and $TE_{4,3,i} \cap ITE_{4,3,2}$ are identical to the models in Fig. 8 (c) and 8(d), respectively. Also, we have $\Pr(SR|TE_{4,3,i} \cap ITE_{4,3,m}) = CR_{TE_{4,3,i}\cap ITE_{4,3,m}}(t) \times P_{u-TE_{4,3,i}\cap ITE_{4,3,m}}(t)$ with $CR_{TE_{4,3,i}\cap ITE_{4,3,m}}(t)$ and $P_{u-TE_{4,3,i}\cap ITE_{4,3,m}}(t)$ summarized in Table 14.

$TE_{4,4,i}$: The reduced system FT model under $TE_{4,4,i}$ is generated by removing all the relay failure events and the FDEP gates from the dynamic FT of the example BSN system and replacing S_2 and S_3 with '1', which is identical to that under $TE_{4,1} \cap ITE_{4,1,4}$ (Fig. 8(d)). Therefore, $CR_{TE_{4,4,i}}(t) = 0$, resulting in $\Pr(SR|TE_{4,4,i}) = CR_{TE_{4,4,i}}(t) \times P_{u-TE_{4,4,i}}(t) = 0$.

4.2.5. Step 5: integrate for the entire BSN system reliability

In Step 3, according to (20), we integrate $\Pr(SR \cap TE_1)$ with $\Pr(TE_1)$ and $\Pr(SR|TE_1)$ evaluated by (21) and (22). According to (25), we integrate $\Pr(SR \cap TE_2)$ with $\Pr(SR|TE_2)$ and $\Pr(TE_2)$. According to (26), we integrate $\Pr(SR \cap TE_3)$ with $\Pr(SR \cap TE_{3,1})$ and $\Pr(SR \cap TE_{3,2})$ evaluated by (27) and (30). And according to (32), we integrate $\Pr(SR \cap TE_4)$ with $\Pr(SR \cap TE_{4,k}), k = 1,2,3,4$ evaluated by (33), (35), (38), and (39). In Step 2, we integrate $CR(t)$ with $\Pr(SR \cap TE_j), j = 1,2,3,4$. According to (6), we integrate the example BSN reliability, $R_{BSN}(t)$, with $P_u(t)$ evaluated by (18) and $CR(t)$ evaluated by (19).

Table 15
Time-to-LF/PFGE parameters of the example BSN biosensors.

Biosensor	Set 1 (Exponential)		Set 2 (Weibull)	
	α_{iLF}/hrs	α_{iPF}/hrs	(α_{iLF}/hrs, β_{iLF})	(α_{iPF}/hrs, β_{iPF})
S_1	2.78e-3	5.00e-5	(2.78e-3, 1.0)	(5.00e-5, 2.0)
S_2	4.17e-3	5.00e-5	(4.17e-3, 2.0)	(5.00e-5, 2.5)
S_3	4.17e-3	5.00e-5	(4.17e-3, 1.5)	(5.00e-5, 1.7)
R_1	5.21e-3	1.00e-4	(5.21e-3, 2.3)	(1.00e-4, 1.2)
R_2	8.33e-3	1.00e-4	(8.33e-3, 2.5)	(1.00e-4, 3.0)

5. Numerical results and analysis

The Weibull distribution with the scale parameter (α) and the shape parameter (β) is adopted for modeling biosensors' time-to-LF/PFGE and isolation time (IT) [13]. The PDF of random variable W with the Weibull distribution is given as (42). Particularly, the Weibull distribution reduces to the exponential distribution when $\beta = 1$. Table 15 illustrates the values of input time-to-LF/PFGE parameters.

$$f_W(t) = \beta\alpha^{\beta} t^{(\beta-1)} e^{-(\alpha t)^{\beta}} \tag{42}$$

Note that in this paper, we have focused on system-level reliability modeling and evaluation with the assumption that these component-level failure parameters are known input parameters. In practice, estimation approaches based on collected failure data (e.g., statistical inference [52], Bayesian estimation [53]) are often applied to estimate component failure time distribution functions and related parameters.

In this work, we discuss the IT performance of the dependent biosensors (i.e., S_2 and S_3) on the reliability of the example BSN system based on the different relationships between LF and PFGE of the same biosensor (*s*-independent in Section 5.1 and disjoint in Section 5.2). The analysis of the results is performed in Section 5.3. In Section 5.4, the correctness of the proposed method is verified using the continuous-time Markov chains (CTMC) method.

5.1. Impact of isolation time under the s-independent relationship

Using parameters of Set 1, Table 16 presents the BSN reliabilities at different mission time (t = 24, 48, and 72 h) when S_2IT and S_3IT follow the exponential distribution with changing scale parameters (α_{S_2IT} and α_{S_3IT}).

Using parameters of Set 2, Tables 17 and 18 present the BSN reliabilities when S_2IT and S_3IT follow the Weibull distribution. Specifically, Table 17 addresses the impact of S_2IT (α_{S_2IT}, β_{S_2IT}) where S_3IT is fixed as (α_{S_3IT},β_{S_3IT})=(8.33e-3/hour, 1). Table 18 addresses the impact of

Table 16
Impacts of α_{S_2IT} and α_{S_3IT} on R_{BSN} under Set 1 (Exponential).

t (hrs)	α_{S_2IT}	α_{S_3IT}			
		3600	1	8.33e-3	1.00e-9
24	3600	0.929843	0.931317	0.965033	0.968801
	1	0.931170	0.932355	0.965303	0.969009
	1.04e-2	0.946274	0.947182	0.968927	0.971383
	1.00e-9	0.947729	0.948631	0.969301	0.971612
48	3600	0.794125	0.795915	0.879594	0.899225
	1	0.795918	0.797398	0.880255	0.899757
	1.04e-2	0.837388	0.838565	0.897908	0.912073
	1.00e-9	0.845558	0.846729	0.901613	0.914501
72	3600	0.645589	0.647226	0.762896	0.806354
	1	0.647384	0.648774	0.763806	0.807109
	1.04e-2	0.709753	0.710898	0.799430	0.833381
	1.00e-9	0.729170	0.730309	0.811154	0.841565

Table 17
Impacts of (α_{S_2IT}, β_{S_2IT}) on R_{BSN} under Set 2 (Weibull) with (α_{S_3IT}, β_{S_3IT})=(8.33e-3, 1).

t (hrs)	α_{S_2IT}	β_{S_2IT}			
		0.5	1.0	1.5	2.0
24	3600	0.99625759	0.99625759	0.99625759	0.99625759
	1	0.99626165	0.99626057	0.99626038	0.99626035
	1.04e-2	0.99627417	0.99627683	0.99627751	0.99627769
	1.00e-9	0.99627777	0.99627777	0.99627777	0.99627777
48	3600	0.97778415	0.97778412	0.97778412	0.97778412
	1	0.97790569	0.97786070	0.97785454	0.97785361
	1.04e-2	0.97852760	0.97867541	0.97872813	0.97874813
	1.00e-9	0.97876260	0.97876268	0.97876268	0.97876268
72	3600	0.93013347	0.93013335	0.93013334	0.93013334
	1	0.93084126	0.93054733	0.93051130	0.93050555
	1.04e-2	0.93586248	0.93711128	0.93764795	0.93789459
	1.00e-9	0.93816123	0.93816210	0.93816210	0.93816210

Table 18
Impacts of (α_{S_3IT}, β_{S_3IT}) on R_{BSN} under Set 2 (Weibull) with (α_{S_2IT}, β_{S_2IT})=(1.04e-2, 1).

t (hrs)	α_{S_3IT}	β_{S_3IT}			
		0.5	1.0	1.5	2.0
24	3600	0.99508553	0.99508549	0.99508549	0.99508567
	1	0.99527294	0.99520745	0.99519790	0.99519648
	8.33e-3	0.99610152	0.99627683	0.99632557	0.99633970
	1.00e-9	0.99634600	0.99634610	0.99634610	0.99634609
48	3600	0.96639659	0.96639640	0.96639638	0.96639638
	1	0.96754405	0.96705044	0.96699188	0.96698237
	8.33e-3	0.97652341	0.97867541	0.97952194	0.97987073
	1.00e-9	0.98015184	0.98015334	0.98015334	0.98015333
72	3600	0.89507901	0.89507860	0.89507856	0.89507855
	1	0.89779649	0.89652825	0.89639152	0.89636863
	8.33e-3	0.92924305	0.93711128	0.94087306	0.94276758
	1.00e-9	0.94513426	0.94514111	0.94514112	0.94514111

S_3IT (α_{S_3IT}, β_{S_3IT}) where S_2IT is fixed as (α_{S_2IT}, β_{S_2IT})=(1.04e-2/hour, 1).

5.2. Impact of isolation time under the disjoint relationship

Using the same parameters as those in Section 5.1, the BSN reliabilities for disjoint LF and PFGE are collected in Tables 19–21.

5.3. Analysis of numerical results

5.3.1. Scale parameter analysis

It can be seen from Tables 16–21 that, when the shape parameters are fixed, the example BSN reliability (R_{BSN}) shows a growing trend as the scale parameters of S_2IT and S_3IT (α_{S_2IT} and α_{S_3IT}) decrease. This phenomenon demonstrates that, compared with the improvement effect of the failure isolation, the deterioration effect caused by the same failure isolation dominates the system performance. Specifically, the failure isolation of S_2 and S_3 leads to a two-sided effect on system performance: preventing PFGEs of S_2 and S_3 from affecting other parts of the BSN system (the improvement effect); meanwhile, S_2 and S_3 becoming inaccessible (the deterioration effect). In the example BSN system with considered parameter settings, when α_{S_2IT} and α_{S_3IT} increase, the isolation probabilities of S_2 and S_3 are increasing, i.e., there are more likely for S_2 and S_3 to be isolated from the BSN system when relays fail. As the deterioration effect is dominating, the BSN system performance becomes worse.

5.3.2. Shape parameter analysis

The impact of the shape parameter on the example BSN reliability is less obvious than that of the scale parameter. In the extreme cases, where α_{S_2IT} and α_{S_3IT} are 1.0e-9/hours or 3600/hours (corresponding to the case that biosensors take almost infinite or instant time to be isolated), the impact of β_{S_2IT} and β_{S_3IT} on the BSN reliability is trivial for the considered parameter settings.

In addition, the example BSN reliability's trend as the shape parameter ($\beta_{S_2IT}/\beta_{S_3IT}$) increases depends on the value of the scale parameter. Take results at t = 48 h in Tables 17 and 18 as examples. Fig. 9 depicts how the BSN reliability changes as β_{S_2IT} and β_{S_3IT} increase from 0.5 to 2.0. When the scale parameter (α) is 1/hour, the example BSN reliability decreases as the shape parameter (β) increases; whereas, when α is 1.04e-2/hour or 8.33e-3/hour, the example BSN reliability increases as β increases. This phenomenon is caused by the dominating deterioration effect. When α is 1/hour, the isolation probability increases with increasing β, i.e., it is more likely that dependent biosensors are isolated from the BSN system. As the deterioration effect dominates, the BSN system performs worse. When α is 1.04e-2/hour or 8.33e-3/hour, the isolation probability decreases with increasing β, leading to a better reliability performance of the example BSN system.

5.3.3. LF and PFGE relationship impact

Results show that the BSN reliability under the case of LF and PFGE being s-independent is higher than that under the case of LF and PFGE being disjoint. For example, using the parameters given in Set 1 and (α_{S_2IT}, α_{S_3IT}) = (3600/hour, 3600/hour), the system reliability is 0.929843 under the s-independent relationship (in the cell marked with shadow of Table 16) and is 0.929633 under the disjoint relationship (in the cell marked with shadow of Table 19). This is because the

Table 19
Impacts of α_{S_2IT} and α_{S_3IT} on R_{BSN} under Set 1 (Exponential).

t (hrs)	α_{S_2IT}	α_{S_3IT}			
		3600	1	8.33e-3	1.00e-9
24	3600	0.929633	0.931117	0.964959	0.968738
	1	0.930970	0.932162	0.965231	0.968948
	1.04e-2	0.946141	0.947055	0.968873	0.971335
	1.00e-9	0.947601	0.948509	0.969248	0.971565
48	3600	0.792930	0.794742	0.879009	0.898743
	1	0.794748	0.796246	0.879681	0.899284
	1.04e-2	0.836590	0.837781	0.897508	0.911740
	1.00e-9	0.844813	0.845997	0.901241	0.914189
72	3600	0.642705	0.644372	0.761167	0.804916
	1	0.644537	0.645953	0.762098	0.805689
	1.04e-2	0.707732	0.708898	0.798240	0.832401

Table 20
Impacts of $(\alpha_{S_2IT}, \beta_{S_2IT})$ on R_{BSN} under Set 2 (Weibull) with $(\alpha_{S_3IT}, \beta_{S_3IT})$=(8.33e-3, 1).

t (hrs)	α_{S_2IT}	β_{S_2IT} 0.5	1.0	1.5	2.0
24	3600	0.99625755	0.99625755	0.99625755	0.99625755
	1	0.99626161	0.99626053	0.99626034	0.99626031
	1.04e-2	0.99627414	0.99627680	0.99627748	0.99627766
	1.00e-9	0.99627774	0.99627774	0.99627774	0.9962774
48	3600	0.97778197	0.97778195	0.97778194	0.97778194
	1	0.97790375	0.97785869	0.97785251	0.97785158
	1.04e-2	0.97852669	0.97867474	0.97872753	0.97874756
	1.00e-9	0.97876205	0.97876213	0.97876213	0.97876213
72	3600	0.93010875	0.93010863	0.93010862	0.93010862
	1	0.93081889	0.93052405	0.93048791	0.93048214
	1.04e-2	0.93585381	0.93710593	0.93764391	0.93789110
	1.00e-9	0.93815824	0.93815911	0.93815911	0.93815911

Table 21
Impacts of $(\alpha_{S_3IT}, \beta_{S_3IT})$ on R_{BSN} under Set 2 (Weibull) with $(\alpha_{S_2IT}, \beta_{S_2IT})$=(1.04e-2, 1).

t (hrs)	α_{S_3IT}	β_{S_3IT} 0.5	1.0	1.5	2.0
24	3600	0.99508550	0.99508546	0.99508546	0.99508546
	1	0.99527291	0.99520742	0.99519787	0.99519645
	8.33e-3	0.99610149	0.99627680	0.99632554	0.99633967
	1.00e-9	0.99634598	0.99634607	0.99634607	0.99634606
48	3600	0.96639565	0.96639547	0.96639545	0.96639545
	1	0.96754312	0.96704950	0.96699095	0.96698143
	8.33e-3	0.97652269	0.97867474	0.97952129	0.97987009
	1.00e-9	0.98015121	0.98015271	0.98015271	0.98015270
72	3600	0.89507121	0.89507080	0.89507076	0.89507076
	1	0.89778874	0.89652045	0.89638372	0.89636084
	8.33e-3	0.92923720	0.93710593	0.94086799	0.94276266
	1.00e-9	0.94512953	0.94513638	0.94513638	0.94513638

biosensor's reliability (i.e., the occurrence probability that biosensor experiences neither LFs nor PFGEs) under the *s*-independent case (calculated as $[1 - q_{iLF}(t)] \times [1 - q_{iPF}(t)]$ for biosensor *i*) is higher than that under the disjoint case (calculated as $[1 - q_{iLF}(t) - q_{iPF}(t)]$).

5.3.4. System reliability's sensitivity to S_2IT and S_3IT

Take the impact of α_{S_2IT} and α_{S_3IT} as illustration. In Table 16, at $t =$ 72 h and α_{S_3IT}=1.00e-9/hour, changing α_{S_2IT} from 3600/hour to 1.00e-9/hour, the BSN reliability increases by 4.37% (computed as (0.841565–0.806354)/0.806354 × 100%); however, at α_{S_2IT}=1.00e-9/hour, taking the same decrement of α_{S_3IT}, the BSN reliability increases by 15.41% (computed as (0.841565–0.729170)/0.729170 × 100%).

The reason of this phenomenon is that isolating S_2 requires both R_1 and R_2 to fail whereas isolating S_3 only requires R_2 to fail, i.e., S_3 is more easily isolated from the example BSN system. Take an extreme case where R_1 is assumed being perfect (i.e., R_1 is replaced by '0' in Fig. 5) as an example. The battery of S_2 is impossible to support the direct communication between S_2 and the sink device; however, the battery of S_3 may be sufficient to support the direct communication once R_2 fails locally. In this extreme case, the example BSN performance is not affected by the IT parameters of S_2 but is by the IT parameters of S_3. In summary, for the example BSN system, the BSN reliability is more sensitive to the IT parameters of S_3 than S_2.

5.4. Verification

To verify the correctness of the proposed method, we use a special case of the example BSN system that can be analyzed using the CTMC method.

The special case requires that parameters of Set 1 (Exponential distribution) are used, LF and PFGE of the same biosensor are *s*-independent, and the isolation of the dependent biosensor upon the LFs of relays is instantaneous (by setting $\alpha_{S_2IT} = 1.00e5/hour$ and $\alpha_{S_3IT} = 1.00e5/hour$). To reduce the size of CTMC, we set PFGE parameters of NDCs to be 0, i.e., $\alpha_{S_1PF} = 0$, $\alpha_{R_1PF} = 0$, and $\alpha_{R_2PF} = 0$. Fig. 10 shows the Markov model for the example BSN system.

Using the Laplace transform-based method, we obtain the BSN reliability as 0.935438 at $t = 24$ h, which exactly matches the result obtained using the proposed method.

Note that the CTMC-based method cannot analyze cases where the LF and PFGE of the same biosensor are dependent or disjoint. Moreover, the CTMC-based method is limited to the exponential distribution and has the size explosion issue (its model size grows exponentially with the number of system components). In contrast, the proposed approach has no limitation on the types of distributions characterizing biosensors' time-to-LF/PFGE and isolation time. In addition, the proposed approach practices the "divide-and-conquer" strategy to decompose the original complex reliability problem into independent reduced problems that can be analyzed in parallel, given available computing resources.

6. Conclusion and future work

This work proposes a combinatorial and analytical method for the reliability analysis of BSNs with multiple correlated FDEP groups and random isolation time. The proposed method is a five-step procedure, which practices the divide-and-conquer principle to decompose a complex reliability problem into several reduced problems that can be efficiently solved. The proposed method has no limitation on the distribution types of time-to-LF/PFGE and IT of the BSN biosensors. An

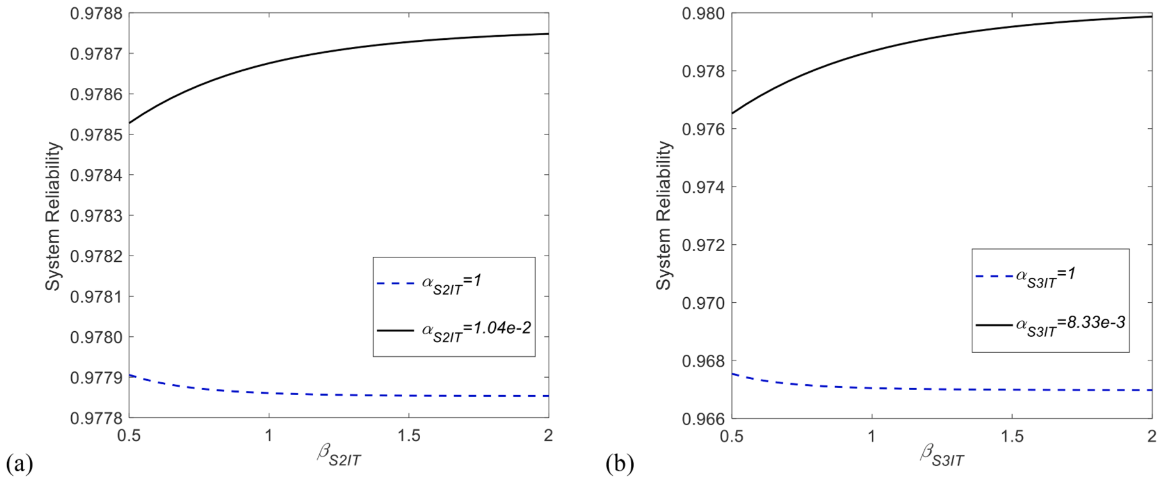

Fig. 9. R_{BSN} under *s*-independent case (a) Impact of $(\alpha_{S_2IT}, \beta_{S_2IT})$ when $(\alpha_{S_3IT}, \beta_{S_3IT})$=(8.33e-3, 1); (b) Impact of $(\alpha_{S_3IT}, \beta_{S_3IT})$ when $(\alpha_{S_2IT}, \beta_{S_2IT})$=(1.04e-2, 1).

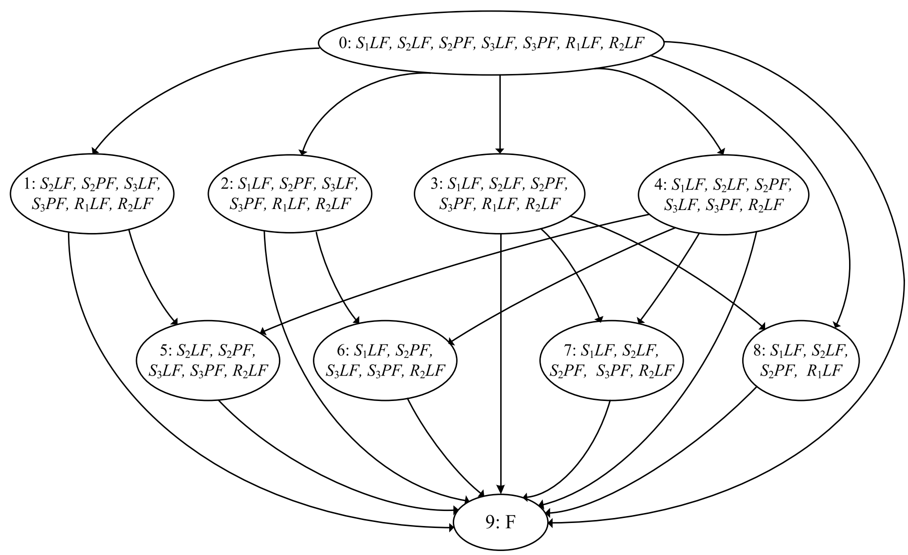

$$\lambda_{0\to1}=\lambda_{S_1LF},\lambda_{0\to2}=\lambda_{S_2LF},\lambda_{0\to3}=\lambda_{S_3LF},\lambda_{0\to4}=\lambda_{R_1LF},\lambda_{0\to8}=\lambda_{R_2LF},\lambda_{0\to9}=\lambda_{S_2PF}+\lambda_{S_3PF}$$
$$\lambda_{1\to5}=\lambda_{R_1LF},\lambda_{1\to9}=\lambda_{S_2LF}+\lambda_{S_2PF}+\lambda_{S_3LF}+\lambda_{S_3PF}+\lambda_{R_2LF}$$
$$\lambda_{2\to6}=\lambda_{R_1LF},\lambda_{2\to9}=\lambda_{S_1LF}+\lambda_{S_2PF}+\lambda_{S_3LF}+\lambda_{S_3PF}+\lambda_{R_2LF}$$
$$\lambda_{3\to7}=\lambda_{R_1LF},\lambda_{3\to8}=\lambda_{R_2LF},\lambda_{3\to9}=\lambda_{S_1LF}+\lambda_{S_2LF}+\lambda_{S_2PF}+\lambda_{S_3PF}$$
$$\lambda_{4\to5}=\lambda_{S_1LF},\lambda_{4\to6}=\lambda_{S_2LF},\lambda_{4\to7}=\lambda_{S_3LF},\lambda_{4\to9}=\lambda_{S_2PF}+\lambda_{S_3PF}+\lambda_{R_2LF}$$
$$\lambda_{5\to9}=\lambda_{S_2LF}+\lambda_{S_2PF}+\lambda_{S_3LF}+\lambda_{S_3PF}+\lambda_{R_2LF},\lambda_{6\to9}=\lambda_{S_1LF}+\lambda_{S_2PF}+\lambda_{S_3LF}+\lambda_{S_3PF}+\lambda_{R_2LF}$$
$$\lambda_{7\to9}=\lambda_{S_1LF}+\lambda_{S_2LF}+\lambda_{S_2PF}+\lambda_{S_3PF}+\lambda_{R_2LF},\lambda_{8\to9}=\lambda_{S_1LF}+\lambda_{S_2LF}+\lambda_{S_2PF}+\lambda_{R_1LF}$$

Fig. 10. Markov model for calculating the example BSN reliability.

example of a BSN system is modeled and analyzed to demonstrate the proposed method and impacts of random isolation time parameters of dependent biosensors. Numerical results reveal that the isolation time parameters, the relationship between LF and PFGE, and the configuration of dependent biosensors can significantly affect the example BSN reliability. The correctness of the method is verified using the CTMC method.

Note that the addressed problem and the proposed solution procedure center around the BSN application. However, the problem of competing with correlated isolation groups and the proposed reliability analysis method are applicable to other applications that adopt relay-based wireless sensor networks to achieve efficient planning and management solutions [41], such as smart homes [54], smart grids [55], intelligent transportation systems [56], etc.

This work assumes that the BSN system and its biosensors have binary states (operation or failure) and are not repairable during the considered mission time. As one direction of the future work, it should be interesting to extend the proposed methodology to consider the repair behavior and the multi-state behavior where both the system and components may have multiple performance levels. Another direction is to model, analyze, and design resilience of BSN systems, which is concerned with the system's ability to survive from failures or hazards [57]. Resilience metrics, models, analysis methods, and design techniques will be explored for BSN systems while considering the competing failure behavior and random isolation time.

CRediT authorship contribution statement

Guilin Zhao: Writing – original draft, Methodology, Funding acquisition. **Liudong Xing:** Writing – review & editing, Supervision, Methodology, Conceptualization.

Declaration of Competing Interest

The authors declare that they have no known competing financial interests or personal relationships that could have appeared to influence the work reported in this paper.

Data availability

No data was used for the research described in the article.

Acknowledgment

The research was supported by the National Natural Science Foundation of China (NSFC) under Grant 62202394.

References

[1] Awotunde JB, Jimoh RG, AbdulRaheem M, Oladipo ID, et al. IoT-based wearable body sensor network for COVID-19 pandemic. In: Hassanien AE, Elghamrawy SM, Zelinka I, editors. Advances in data science and intelligent data communication technologies for COVID-19. studies in systems, decision and control. Cham: Springer; 2022. p. 253–75.
[2] Ali S, Singh R, Javaid M, Haleem A, et al. A review of the role of smart wireless medical sensor network in COVID-19. J Indus Integr Manag 2020;5(4):413. 425.
[3] Ding X, Clifton D, Ji N, Lovell NH, et al. Wearable sensing and telehealth technology with potential applications in the Coronavirus pandemic. IEEE Rev Biomed Eng 2021;14:48–70.
[4] Bilandi N, Verma K, Dhir R. An intelligent and energy-efficient wireless body area network to control Coronavirus outbreak. Arab J Sci Eng 2021;46:8203–22.
[5] Appelboom G, Camacho E, Abraham ME, Dumont EL, et al. Smart wearable body sensors for patient self-assessment and monitoring. Arch Public Health 2014;72 (28).
[6] Waheed M, Ahmad R, Ahmed W, Dridberg M, Alam M. Towards efficient wireless body area network using two-way relay cooperation. Sensors 2018;18(2):565.
[7] Dasgupta A, Mennemanteuil M, Buret M, Cazier N, et al. Optical wireless link between a nanoscale antenna and a transducing rectenna. Nat Commun 2018;9 (1992):1–7.
[8] Park D, Kwak K, Chung WK, Kim J. Development of underwater short-range sensor using electromagnetic wave attenuation. IEEE J Ocean Eng 2016;41(2):318–25.
[9] Levitin G, Xing L. Reliability and performance of multi-state systems with propagated failures having selective effect. Reliab Eng Syst Saf 2010;95(6):655–61.
[10] Xing L, Levitin G. Combinatorial analysis of systems with competing failures subject to failure isolation and propagation effects. Reliab Eng Syst Saf 2010;95 (11):1210–5.
[11] Liu J, Xu X, Han S, Zhang Z, Liu C. Hybrid relay selection and cooperative jamming scheme for secure communication in healthcare-IoT. In: Proc. IEEE Wireless Communications and Networking Conference (WCNC); 2021.
[12] Mkongwa KG, Liu Q, Zhang C, Siddiqui FA. Reliability and quality of service issues in wireless body area networks: a survey. Int J Signal Process Syst 2019;7(1): 26–31.
[13] Wang Y, Xing L, Wang H, Levitin G. Combinatorial analysis of body sensor network subject to probabilistic competing failures. Reliab Eng Syst Saf 2015;142:388–98.
[14] Zeng Y, Sun Y. A reliability modeling method for the system subject to common cause failures and competing failures. Qual Reliab Eng Int 2022;38(5):2533–47.
[15] Cheng Y, Yang L, Ye C, Kang R. Failure mechanism dependence and reliability evaluation of non-repairable system. Reliab Eng Syst Saf 2015;138:279–83.
[16] Mo H, Xie M, Xing L. Combinatorial competing failure analysis considering random propagation time. In: Proc. Annual Reliability and Maintainability Symposium (RAMS); 2016.
[17] Cha JH, Guida M, Pulcini G. A competing risks model with degradation phenomena and catastrophic failures. Int J Performab Eng 2014;10(1):63–74.
[18] Li WJ, Pham H. Reliability modeling of multi-state degraded systems with multi-competing failures and random shocks. IEEE Trans Reliab 2005;54(2):297–303.
[19] Liu Y, Bai C. Reliability analysis based on dependent competing risk model of imperfect shock model considering changing threshold and degradation process. *in*. In: Proc. of International Conference on Sensing, Diagnostics, Prognostics, and Control; 2019. p. 301–4.
[20] Tang J, Chen C, Huang L. Reliability assessment models for dependent competing failure processes considering correlations between random shocks and degradations. Qual Reliab Eng Int 2018;35(1):179–91.
[21] Che H, Zeng S, Guo J, Wang Y. Reliability modeling for dependent competing failure processes with mutually dependent degradation process and shock process. Reliab Eng Syst Saf 2018;180:168–78.
[22] Moustafa K, Hu Z, Mourelatos ZP, Baseski I, Majcher M. System reliability analysis using component-level and system-level accelerated life testing. Reliab Eng Syst Saf 2021;214:107755.
[23] Klein JP, Basu AP. Weibull accelerated life tests when there are competing causes of failure. Commun Statist Theory Method 2007;10(20):2073–100.
[24] Peng H, Feng Q, Coit DW. Reliability and maintenance modeling for systems subject to multiple dependent competing failure processes. IIE Trans 2010;43(1): 12–22.
[25] Yousefi N, Coit DW, Zhu X. Dynamic maintenance policy for systems with repairable components subject to mutually dependent competing failure processes. Comput Indus Eng 2020;143:106398.
[26] Pham H, Malon DM. Optimal design of systems with competing failure modes. IEEE Trans Reliab 1994;43(2):251–4.
[27] Song S, Coit DW, Feng Q, Peng H. Reliability analysis for multi-component systems subject to multiple dependent competing failure processes. IEEE Trans Reliab 2014;63(1):331–45.
[28] Myers AF. k-out-of-n: g system reliability with imperfect fault coverage. IEEE Trans Reliab 2007;56(3):464–73.
[29] Xing L. Reliability evaluation of phased-mission systems with imperfect fault coverage and common-cause failures. IEEE Trans Reliab 2007;56(1):58–68.
[30] Xiang J, Machida F, Tadano K, Maeno Y. An imperfect fault coverage model with coverage of irrelevant components. IEEE Trans Reliab 2015;64(1):320–32.
[31] Wang C, Xing L, Weng J. A new combinatorial model for deterministic competing failure analysis. Qual Reliab Eng Int 2020;36(5):1475–93.
[32] Wang Y, Xing L, Wang H. Reliability of systems subject to competing failure propagation and probabilistic failure isolation. Int J Syst Sci: Oper Logist 2017;4 (3):241–59.
[33] Wang C, Liu Q, Xing L, Guan Q, et al. Reliability analysis of smart home sensor systems subject to competing failures. Reliab Eng Syst Saf 2022;221:108327.
[34] Xing L, Levitin G. Combinatorial algorithm for reliability analysis of multi-state systems with propagated failures and failure isolation effect. IEEE Transact Syst Man Cybernet Part A: Syst Hum 2011;41(6):1156–65.
[35] Wang C, Xing L, Peng R, Pan Z. Competing failure analysis in phased-mission systems with multiple functional dependence groups. Reliab Eng Syst Saf 2017; 164:24–33.
[36] Wang Y, Xing L, Levitin G, Huang N. Probabilistic competing failure analysis in phased-mission systems. Reliab Eng Syst Saf 2018;176:37–51.
[37] Xing L, Zhao G, Xiang YS, Liu Q. A behavior-driven reliability modeling method for complex smart systems. Qual Reliab Eng Int 2021;37(5):2065–84.
[38] Zhao G, Xing L. Competing failure analysis considering cascading functional dependence & random failure propagation time. Qual Reliab Eng Int 2019;35(7): 2327–42.
[39] Zhao G, Xing L. Competing failure analysis in IoT systems with cascading probabilistic function dependence. Reliab Eng Syst Saf 2020;198:106812.
[40] Zhao G, Xing L. Reliability analysis of body sensor networks subject to random isolation time. Reliab Eng Syst Saf 2021;207:107345.
[41] Xing L. Reliability in Internet of things: current status and future perspectives. IEEE Internet of Things J 2020;7(8):6704–21.
[42] Roscoe K, F Diermanse, Vrouwenvelder T. System reliability with correlated components: accuracy of the equivalent planes method. Struct Saf 2015;57:53–64.
[43] Wang Y, Xing L, Wang H, Coit DW. System reliability modeling considering correlated probabilistic competing failures. IEEE Trans Reliab 2018;67(2):416–31.
[44] Long W, Sato Y, Horigome M. Quantification of sequential failure logic for fault tree analysis. Reliab Eng Sys Saf 2000;67(3):269–74.
[45] Naresky JJ. Reliability Definitions. IEEE Trans Reliab 1970;R-19(4):198–200.
[46] C. Therrien and M. Tummala, *Probability and random processes for electrical and computer engineers*, CRC Press, ISBN: 978–1439826980.
[47] Xing L, Amari SV. Binary decision diagrams and extensions for system reliability analysis. MA: Wiley-Scrivener; 2015. ISBN: 978-1-118-54937-7.
[48] Yevkin O. An efficient approximate Markov chain method in dynamic fault tree analysis. Qual Reliab Eng Int 2015;32(4):1509–20.
[49] Durga Rao K, Gopika V, Sanyasi Rao VVS, Kushwaha HS, et al. Dynamic fault tree analysis using Monte Carlo simulation in probabilistic safety assessment. Reliab Eng Syst Saf 2009;94(3):872–83.
[50] Zhu P, Han J, Liu L, Lombardi F. A stochastic approach for the analysis of dynamic fault trees with spare gates under probabilistic common cause failures. IEEE Trans Reliab 2015;64(3):878–92.
[51] Jiang G, Yuan H, Li P, Li P. A new approach to fuzzy dynamic fault tree analysis using the weakest n-dimensional t-norm arithmetic. Chin J Aeronaut 2018;31(7): 1506–14.
[52] Allen A. Probability, statistics and queuing theory: with computer science applications. 2nd editor. New York: Academic; 1991. ISBN: 0120510510.
[53] Dellaportas P, Wright DE. Numerical prediction for the 2-parameter Weibull distribution. The Statistician 1991;40(4):365–72.
[54] Chhaya L, Sharma P, Bhagwatikar G, Kumar A. Wireless sensor network based smart grid communications: cyber attacks, intrusion detection system and topology control. Electronics (Basel) 2017;6(5):1–22.
[55] Rajaram ML, Kougianos E, Mohanty SP, Sundaravadivel P. A wireless sensor network simulation framework for structural health monitoring in smart cities. In:

IEEE 6th International Conference on Consumer Electronics - Berlin (ICCE-Berlin); 2016.
[56] Tubaishat M, Zhuang P, Qi Q, Shang Y. Wireless sensor networks in intelligent transportation systems. Wirel Commun Mob Comput 2009;9:287–302.
[57] Xing L. Cascading failures in Internet of things: review and perspectives on reliability and resilience. IEEE Internet of Things J 2021;8(1):44–64.